Tampere University

Kristian Asti

NUMERICAL APPROXIMATION OF DYNAMIC EULER–BERNOULLI BEAMS AND A FLEXIBLE SATELLITE

Master of Science Thesis, 63 pages, 0 Appendix pages
Faculty of Information Technology and Communication Sciences
Examiners: Associate Professor Lassi Paunonen
Post-Doctoral Research Fellow Jukka-Pekka Humaloja
August 2020

ABSTRACT

Kristian Asti: Numerical Approximation of Dynamic Euler–Bernoulli Beams and a Flexible Satellite
Master of Science Thesis, 63 pages, 0 Appendix pages
Tampere University
Degree Programme in Science and Engineering
Main subject: Mathematics
August 2020

In this work, we develop a numerical method for simulating Euler–Bernoulli beams. We use this method for simulating a single beam, as well as simulating the solar panels of a flexible satellite. In developing the method, we apply mathematical control theory, Legendre polynomials, Fourier–Legendre series expansion and the spectral Galerkin method.

The main goal of this work is to develop a numerical model that we can use for doing simulations in MATLAB. We obtain a linear system of first-order differential equations, which we can solve with dedicated tools. We included the possibility to apply time-dependent boundary control input in the simulation model developed for a single beam. This allows us to use this model in simulating a flexible satellite. In the approximate model for the flexible satellite, we included the possibility to apply time-dependent control input to the system.

We study the existence of solutions to the dynamic beam equation with homogeneous boundary conditions (i.e. without boundary control input) by applying mathematical control theory and the theory of strongly continuous semigroups in particular. This is not a central part of the work, but we include it as a theoretical foundation for the existence of numerical solutions to the beam equation. As an introduction, we study boundary conditions corresponding to differently mounted beams with static beams first. Boundary conditions corresponding to different beam mountings form an essential part of solving the beam equation and developing the numerical method.

The numerical approximation for beams is based on modal basis functions made of Legendre polynomials and the spectral Galerkin method utilising these polynomials. The Legendre polynomials are computationally well applicable, as they are polynomials with integer coefficients and thus can be represented numerically as coefficient vectors to a high precision. Operations between these polynomials are also computationally simple. The use of Legendre polynomials is further motivated by the fact that they are great for approximating continuously differentiable functions.

The model for a flexible satellite consists of a small, rigid central body and two identical flexible solar panels, which we model as dynamic Euler–Bernoulli beams. The solar panels are mounted symmetrically to the central body and they affect each other via the boundary mountings. We model the satellite numerically by applying the approximate model developed for a single beam to both solar panels, and using a model derived from Newton's laws for the central body. Using the boundary connections between the components, we combine the three systems into a single system, which we can simulate using MATLAB.

Keywords: Euler–Bernoulli beam theory, beam equation, Legendre polynomials, spectral method, Galerkin method, boundary control, flexible satellite, control theory

TIIVISTELMÄ

Kristian Asti: Dynaamisten Euler–Bernoulli-palkkien ja taipuisan satelliitin numeerinen approksimointi
Diplomityö, 63 sivua, 0 liitesivua
Tampereen yliopisto
Teknis-luonnontieteellinen koulutusohjelma
Pääaine: Matematiikka
Elokuu 2020

Tässä työssä kehitetään numeerinen menetelmä Euler–Bernoulli-palkkien simulointia varten. Tätä menetelmää käytetään paitsi yksittäisen palkin simulointiin, myös taipuisan satelliitin aurinkopaneelien mallintamiseen. Mallin johtamisessa hyödynnetään matemaattista systeemiteoriaa, Legendren polynomeja, Fourier–Legendren sarjakehitelmää sekä Galerkinin spektraalimenetelmää.

Työn päätavoitteena on kehittää simulointikelpoinen numeerinen malli, jota voidaan käyttää simulaatioiden tekemiseen MATLAB-ohjelmistolla . Tuloksena on lineaarinen ensimmäisen asteen differentiaaliyhtälösysteemi, joka on ratkaistavissa siihen kehitetyillä työkaluilla. Yhden palkin simulointimalliin on sisällytetty mahdollisuus käyttää ajasta riippuvaa reunaohjaussignaalia, mikä mahdollistaa sen soveltamisen satelliittimallissamme. Vastaavasti taipuisan satelliitin malliin on sisällytetty mahdollisuus käyttää ajasta riippuvaa ohjaussignaalia.

Aikariippuvan palkkiyhtälön ratkaisujen olemassaoloa homogeenisille reunaehdoille (ilman reunaohjaussignaalia) tutkitaan matemaattisen systeemiteorian ja erityisesti vahvasti jatkuvien puoliryhmien teorian avulla. Tämä ei ole keskeinen osa työtä, mutta sisällytetään eräänlaisena teoreettisena perustana palkkiyhtälön numeeristen ratkaisujen olemassaololle. Eri tavoilla kiinnitettyihin palkkeihin liittyviä reunaehtoja tutkitaan johdatuksenomaisesti ensin staattisten palkkien avulla. Erilaisiin palkkikiinnityksiin liittyvät reunaehdot ovat keskeisessä osassa palkkiyhtälön ratkaisemisessa sekä numeerisen menetelmän kehittämisessä.

Varsinainen numeerinen palkkiapproksimaatio rakentuu Legendren polynomeista muodostettujen modaalisista kantafunktioista sekä Galerkinin spektraalimenetelmästä käyttäen näitä polynomeja. Legendren polynomit ovat laskennallisesti hyvin käyttökelpoisia, sillä ne ovat kokonaislukukertoimisina polynomeina esitettävissä numeerisesti kerroinvektorimuodossa suurella tarkkuudella. Operaatiot näiden polynomien kesken ovat niin ikään laskennallisesti yksinkertaisia toteuttaa. Legendren polynomien käyttöä motivoi myös niiden hyvä soveltuvuus jatkuvasti derivoituvien funktioiden approksimointiin.

Taipuisan satelliitin malli koostuu jäykästä, kooltaan pienestä keskuskappaleesta sekä kahdesta identtisestä, taipuisasta aurinkopaneelista, joita mallinnetaan dynaamisina Euler–Bernoulli-palkkeina. Aurinkopaneelit kiinnittyvät symmetrisesti keskuskappaleeseen, ja ne vaikuttavat toisiinsa reunakiinnitysten kautta. Satelliittia mallinnetaan numeerisesti hyödyntämällä yksittäiselle palkille kehitettyä approksimaatiomallia molemmille aurinkopaneeleille ja käyttämällä Newtonin laeista johdettua mallia keskuskappaleelle. Näistä kolmesta systeemistä muodostetaan reunakytkentöjen avulla yksi systeemi, jota voidaan simuloida MATLAB-ohjelmistolla.

Avainsanat: Euler–Bernoulli-palkkiteoria, palkkiyhtälö, Legendren polynomit, spektraalimenetelmä, Galerkinin menetelmä, reunaohjaus, taipuisa satelliitti, systeemiteoria

PREFACE

This work was written as part of the Systems Theory Research Group in Tampere University. The main motivators were the need to be able to numerically simulate a flexible satellite, which is being studied in the research group, and my personal interest in mathematical modelling and numerical simulations. First of all, I would like to thank my supervisor Lassi Paunonen for introducing me to this topic and offering me a Master's Thesis position in the research group. I learned a lot during the course of working on the thesis.

Further thanks go to all my co-workers in the Systems Theory Research Group, who were all extremely welcoming and supportive right from the beginning. Special thanks go to Konsta Huhtala and Jukka-Pekka Humaloja, who were tireless to answer all the numerous questions I had, whether they were related to my thesis topic, systems theory or mathematics in general. I also want to thank Thavamani Govindaraj, who was happy to teach me about the satellite model in a very understandable way.

Finally, I want to express my deep gratitude to all the people close to me for their invaluable support during my studies and especially the year 2020.

Tampere, 13th August 2020

Kristian Asti

CONTENTS

1 Introduction 1
2 Preliminaries 4
2.1 Matrix Exponential Function 4
2.2 Strongly Continuous Semigroups 5
2.3 Abstract Differential Equations 5
2.4 Contraction Semigroups 6
2.5 Legendre Polynomials 7
3 Euler–Bernoulli Beam Theory 15
3.1 Static Beam Equation 15
3.2 Boundary Conditions for Beams 16
3.3 Types of Beams and Examples 17
3.4 Dynamic Beam Equation 19
3.5 Solution via Separation of Variables 20
3.6 Energy Space Formulation 22
3.7 Generation of Contraction Semigroups 24
4 Spectral Galerkin Method for One Euler–Bernoulli Beam 29
4.1 Weighted Residual Methods and Modal Basis Functions 29
4.2 Semidiscretisation of the Energy Space Formulation 31
4.3 Simply Supported Beam with Boundary Control 35
4.4 Cantilevered Beam with Boundary Control 37
4.5 Modal Basis Functions Utilising Legendre Polynomials 39
4.6 Simulation Example for a Single Beam 44
5 Satellite Model Approximation 47
5.1 Satellite Model Setup 47
5.2 Finding Required Basis Functions 48
5.3 Satellite Model as a Linear Matrix System 54
5.4 Simulation Example for a Flexible Satellite 57
5.5 Matlab Codes for the Satellite Approximation 58
6 Conclusions 60
References 62

LIST OF FIGURES

1.1 A vibrating beam rigidly attached to a wall with exaggerated deflection. . . . 1
1.2 The satellite model showing the interaction between the flexible solar panels and the rigid central body through the boundary. 2

2.1 The first six Legendre polynomials. 11

3.1 Mathematical beam Ω in the ξw-plane. 15
3.2 The solution to example 3.1. 18
3.3 The solution to example 3.2. 18

4.1 The first six basis functions of the form $L_k - \frac{4k+10}{2k+7}L_{k+2} + \frac{2k+3}{2k+7}L_{k+4}$. 31
4.2 A cantilevered beam without boundary control input. 45
4.3 A cantilevered beam with boundary control input $\rho a \frac{\partial x_1}{\partial t}(0,t) = -\sin(2\pi t)$. . 46

5.1 A satellite with two flexible solar panels and a rigid central body. 47
5.2 The rigid central body satellite without control inputs. 58
5.3 The rigid central body with control input functions $u_1(t) = -\cos(2\pi t)$ and $u_2(t) = \frac{1}{4}\sin(\pi t)$. 58
5.4 The two flexible solar panels with no control inputs. 59
5.5 The two flexible solar panels with control input functions $u_1(t) = -\cos(2\pi t)$ and $u_2(t) = \frac{1}{4}\sin(\pi t)$. 59

LIST OF SYMBOLS AND ABBREVIATIONS

$\sim$	Asymptotically equal to
$\|x\|_X$	Norm of $x \in X$
$\langle x, y \rangle_X$	Inner product of $x, y \in X$
a	Cross-sectional area
$A, B, C, \ldots$	Matrices, operators
A^{-1}	Inverse of matrix A
A^{T}	Transpose of matrix A
A^*	Conjugate transpose of matrix A
$\mathbb{C}$	Set of complex numbers
$C^n(\Omega; \mathbb{R})$	Set of n times continuously differentiable real functions on Ω
$\mathcal{D}(A)$	Domain of operator A
δ_{ij}	Kronecker delta function, $i, j \in \mathbb{N}$
$\frac{df}{dx}$	Derivative of f with respect to x
$\frac{d^n f}{dx^n}$	n-th derivative of f with respect to x
$\mathrm{diag}(a_1, a_2, ..., a_n)$	Diagonal matrix with diagonal elements a_i
$\frac{\partial f}{\partial x_j}$	Partial derivative of f with respect to x_j
$\frac{\partial^n f}{\partial x_j^n}$	n-th order partial derivative of f with respect to x_j
$\frac{\partial^2 f}{\partial x_k \partial x_j}$	Second-order partial derivative of f first with respect to x_j then with respect to x_k
E	Elastic modulus
γ	Viscous damping coefficient
I	Identity matrix, identity operator, second moment of area
I_m	Moment of inertia
$L^2(\Omega; \mathbb{R})$	Set of square integrable real functions on Ω
L_n	n-th Legendre polynomial defined on $[0, 1]$
$\mathcal{L}(X)$	Set of bounded linear operators on X
m	Mass
$n!$	Factorial of n
$\mathbb{N}$	Set of natural numbers, $\mathbb{N} = \{0, 1, 2, \ldots\}$

$\binom{n}{k}$	Binomial coefficient, n choose k
Ω	Spatial domain, $\Omega \subset \mathbb{R}$
ϕ, Φ	Modal basis functions
ψ, Ψ	Test functions
$\mathcal{R}(A)$	Range of operator A
$\mathrm{rank}(A)$	Rank of matrix A
$\mathbb{R}$	Set of real numbers
$\mathbb{R}^n$	Set of real (column) vectors of n elements
$\mathbb{R}^{m \times n}$	Set of real matrices of size $m \times n$
ρ	Mass density
t	Time
$T(t)$	Strongly continuous semigroup parametrised by $t \in [0, \infty)$
w	Deflection profile of a beam
ξ	Spatial variable, $\xi \in \Omega$

1 INTRODUCTION

In this work, we develop a numerical method to simulate time-dependent beam structures. When we are interested in studying shape and vibration, any solid object of continuous material that is predominantly one-dimensional can be thought of as a beam. Examples include structural beams used in construction, such as I-beams, logs and planks. Elementary physics generally models solid structures as rigid objects, meaning they remain undeformed while subjected to force or torque. This assumption is adequate for strong, rigid materials that are resistant to deformations. However, with large scale beam-like structures, the assumption on rigidity is not reasonable anymore, as deformation and bending become significant and cannot be ignored. Too much deformation or bending might cause the beam to stay permanently deformed, losing its structural strength or break altogether, which can be undesirable or dangerous. The study of mechanics of materials addresses problems and analysis of non-rigid solid materials. A good comprehensive introduction to mechanics of materials is given in [7].

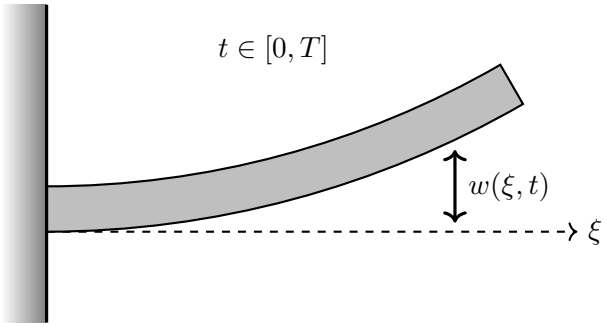

Figure 1.1. *A vibrating beam rigidly attached to a wall with exaggerated deflection.*

The goal of this work is to develop a numerical method to simulate a satellite with flexible solar panels, which we model as Euler–Bernoulli beams. The satellite consists of two identical solar panels attached to a central body, which we model as a rigid particle with negligible dimensions in comparison to the solar panels. We model the solar panels with the time-dependent Euler–Bernoulli beam equation and the central body with a system of two ordinary differential equations. We develop a system of linear ordinary differential equations that approximate the dynamic beam equation. We include time-dependent boundary control input to the approximate beam model, because the two flexible solar panels are connected to the central body via the boundary. We model the satellite as a boundary connected system. We are interested in the movement of the central body caused by the solar panel vibrations and control input to the central body, and the time

evolution of the shape of the solar panels. The satellite model is shown in figure 1.2. The mathematical foundations of the satellite model are covered in [3], [9] and [10].

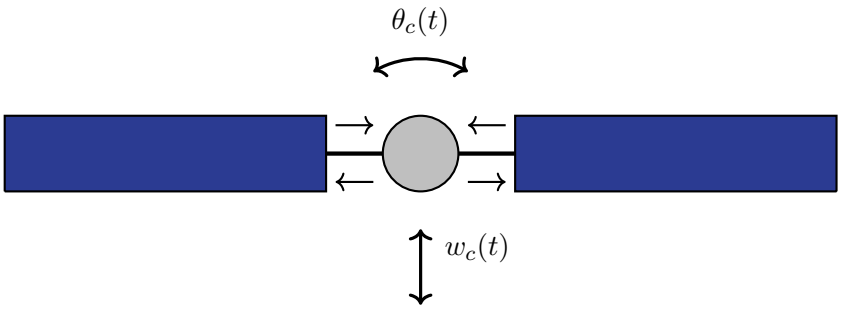

Figure 1.2. *The satellite model showing the interaction between the flexible solar panels and the rigid central body through the boundary.*

In particular, we are interested in theory developed for beams, particularly that developed by Leonhard Euler (1707–1783) and Daniel Bernoulli (1700–1782), also known as the Euler–Bernoulli beam theory. The theory is limited to beams of linearly elastic material with lateral loads only and relatively small bending, and it models only lateral deflections of a beam. For our purposes, this is sufficient, as we apply the theory to model vibrations in the beam caused by elastic potential energy of the beam transforming into kinetic energy and vice versa. Figure 1.1 shows a vibrating team with only lateral deflection.

In the second chapter, we introduce a few concepts that are important in the later work as preliminary knowledge. Strongly continuous semigroups form the background theory for abstract differential equations. For a linear system of first-order ordinary differential equations, the solution can be uniquely expressed, in a theoretical sense, with the matrix exponential function and the initial condition. Further generalising this theory, it can be used to analyse partial differential equations, which can be thought of as infinite-dimensional differential equations. The book [12] is a good introduction to these topics. To the interested reader, [5] offers a more comprehensive approach. We also introduce the Legendre polynomials discovered by Adrien-Marie Legendre (1752–1833). These polynomials are a class of orthogonal polynomials that can be used as a basis for sufficiently smooth functions on $[0, 1]$, and are an essential part of our numerical system.

In the following chapter, we discuss the basics of Euler–Bernoulli beam theory. For a short introduction, we first consider static (time-independent) beams and how different boundary conditions correspond to different beam mountings in real life. From there we proceed to the dynamic beam equation, whose damped version is the core equation for modelling beams and the flexible solar panels in the satellite model. We also present an analytic solution to the equation with homogeneous boundary conditions for completeness. We transform the original fourth-order beam equation into a system of two partial differential equations that are first-order in time, using new state variables. This formulation allows us to apply the theory of port-Hamiltonian systems to analyse the new system. We cover this topic only in a shallow manner, the book [12] offers an introduction to port-Hamiltonian systems.

The fourth chapter contains the main part of this work. Taking the transformed beam equation as our starting point, we study so-called weak solutions to the system. This approach allows us to approximate the system with a system of linear ordinary differential equations by approximating the unknown exact solution with a linear combination of modal basis functions satisfying the required boundary conditions. We apply the weighted residual method and the spectral Galerkin method in this process. These methods and spectral methods more generally are covered, for example, in [17]. We manipulate the weak formulation of the transformed beam system to incorporate boundary control input into the system. A large part of the chapter is dedicated to deriving the matrix formulations for the approximate system of ordinary differential equations describing the beam. We also study how to construct modal basis functions using Legendre polynomials. Last, having all the required tools, we simulate a beam numerically using MATLAB.

In the fifth chapter, we present a mathematical model for the flexible satellite, which consists of two flexible solar panels and a rigid central body. The solar panels are modelled as Euler–Bernoulli beams and the central body is modelled as a point mass. We derive the required modal basis functions using Legendre polynomials to find the matrices for the systems of ordinary differential equations describing the two beams. We then interconnect the two systems for the solar panels and the system describing the motion of the central body to obtain a single system of ordinary differential equations. Similarly to the previous chapter, we simulate the satellite system as the last part of the chapter. In the last chapter, we summarise the simulation model and discuss ways to extend this model to other problems, its weak points and limitations.

The simulation codes developed for MATLAB alongside this work are openly accessible in the writer's GitHub repository at `https://github.com/Kristian-MJA/Satmodel`.

2 PRELIMINARIES

In this work, we assume that the reader is familiar with the core concepts of functional analysis and operator theory. This includes terms such as Banach and Hilbert spaces, L^p-spaces, normed spaces, general inner products, linear operators, bounded operators, compactness, adjoint operators and so on. A good introduction to functional analysis is the book [14].

2.1 Matrix Exponential Function

This section is a brief overview of the matrix exponential on $\mathbb{C}^{n\times n}$. The idea and properties of the matrix exponential will be generalised in the next section in the form of strongly continuous semigroups.

Let A be a complex matrix of size $n \times n$. The matrix exponential is usually defined as

$$e^A := \sum_{n=0}^{\infty} \frac{A^n}{n!}. \tag{2.1}$$

More often, we are interested in the *function* resulting from replacing A by At:

$$e^{At} = \sum_{n=0}^{\infty} \frac{A^n t^n}{n!}, \qquad t \in \mathbb{R}. \tag{2.2}$$

This is usually called the matrix exponential function of A, mapping each real number t to a matrix e^{At}. Additionally, we define e^O (O denotes the zero matrix of size $n \times n$) to equal the identity matrix I of the same size. This is analogous to the convention that $e^0 = 1$ in complex numbers. With this in mind, the matrix exponential function e^{At} can be shown to have the following important properties:

(i) $e^{A0} = e^O = I$

(ii) $e^{A(s+t)} = e^{As}e^{At}$ for all $s, t \in \mathbb{R}$

(iii) the function $t \mapsto e^{At}$ is continuous

(iv) the derivative of e^{At} equals $e^{At}A = Ae^{At}$.

The fourth property in particular is central when solving a system of linear first-order differential equations. Indeed, we could alternatively *define* a mapping that satisfies the properties (i)–(iv) and symbolically denote that by e^{At}, without giving an explicit formula-

tion.

2.2 Strongly Continuous Semigroups

The solution to the initial value problem

$$\frac{d}{dt}x(t) = Ax(t), \qquad x(0) = x_0 \in \mathbb{C}^n, \tag{2.3}$$

where $x\colon [0,\infty) \to \mathbb{C}^n$ and $A \in \mathbb{C}^{n\times n}$, is given by $x(t) = e^{At}x_0$. To analyse infinite-dimensional differential equations of the same form later on, we generalise the idea of the matrix exponential function with a concept possessing similar properties.

Definition 2.1 (Strongly continuous semigroup)**.** Let X be a Hilbert space. We can define a family of operators $(T(t))_{t\geq 0}$ satisfying the following properties:

(i) For all $t \geq 0$, $T(t)$ is linear and bounded, i.e. $T(t) \in \mathcal{L}(X)$

(ii) $T(0) = I$, where $I \in \mathcal{L}(X)$ is the identity operator

(iii) $T(s+t) = T(s)T(t)$ for all $s, t \geq 0$

(iv) the function $t \mapsto T(t)$ satisfies $\lim\limits_{t\to 0+} \|T(t)x - x\|_X = 0$ for all $x \in X$.

A family of operators satisfying (i)–(iv) form a *strongly continuous semigroup* or a C_0-*semigroup*. We call X the *state space* and its elements *states*. Theory on strongly continuous semigroups is covered in, for example, [2, Chapter 5], [5, Chapter 1] and [13, Chapter 1].

The properties (ii) and (iii) are directly analogous to the first two properties of the matrix exponential function. The fourth property is called strong continuity, which is a weaker form of continuity, as opposed to uniform continuity. Requiring the operators to be uniformly continuous would be too restrictive. The matrix exponential function is an example of a strongly continuous semigroup, where $T(t) = e^{At}$ for $t \geq 0$ on the Banach space $\mathbb{C}^n$.

2.3 Abstract Differential Equations

We are now interested in solving the abstract differential equation of the form

$$\frac{d}{dt}x(t) = Ax(t), \qquad x(0) = x_0 \in X. \tag{2.4}$$

Here x generally belongs to an infinite-dimensional vector space such that $t \mapsto x(t) \in X$ for $t \geq 0$ and $A\colon X \to X$ is an operator. The differential equation is not necessarily solvable for an arbitrary operator A. In case of the matrix exponential function, the matrix $A \in \mathbb{C}^{n\times n}$ and the semigroup $(e^{At})_{t\geq 0}$ are linked via the relation $\left(\frac{d}{dt}e^{At}\right)\big|_{t=0} = Ae^{A0} = A$. In a more general case, we wish to find a similar link between an operator A and a

strongly continuous semigroup $(T(t))_{t\geq 0}$. If the following limit exists

$$\lim_{t\to 0+} \frac{T(t)x - x}{t}, \tag{2.5}$$

then x is an element of the domain of A, i.e. $x \in \mathcal{D}(A)$. In this case, we define [12, Definition 5.2.1]

$$Ax = \lim_{t\to 0+} \frac{T(t)x - x}{t}. \tag{2.6}$$

The operator A is called the *infinitesimal generator* of the strongly continuous semigroup $(T(t))_{t\geq 0}$.

The function $t \mapsto T(t)x$ is differentiable for all $x \in \mathcal{D}(A)$, and

$$\frac{d}{dt}\big(T(t)x\big) = T(t)Ax = AT(t)x, \quad t \geq 0. \tag{2.7}$$

Additionally, it can be shown that $T(t)x \in \mathcal{D}(A)$ and A is a closed linear operator [12, Theorem 5.2.2]. We find that if $x_0 \in \mathcal{D}(A)$, the function $x\colon [0,\infty) \to X$, $x(t) = T(t)x_0$ is a solution to (2.4). This is called a *classical solution*. The classical solution is unique for each $x_0 \in \mathcal{D}(A)$ [12, Lemma 5.3.2].

2.4 Contraction Semigroups

Often we only have an abstract differential equation of the form (2.4). In general, there is no guarantee that A is a generator of a C_0-semigroup $(T(t))_{t\geq 0}$. There exist several generation theorems to tackle this problem, but here we only cover contraction semigroups and the Lumer–Phillips Theorem.

Definition 2.2 (Contraction Semigroup)**.** Let $(T(t))_{t\geq 0}$ be a strongly continuous semigroup on a Hilbert space X. If $(T(t))_{t\geq 0}$ satisfies $\|T(t)\|_X \leq 1$ for all $t \geq 0$, we call it a *contraction semigroup.*

The Hille–Yosida Theorem [12, Theorem 6.1.3] states necessary and sufficient conditions for a closed, densely defined and linear operator to be the infinitesimal generator of a contraction semigroup. However, this requires all the powers of the resolvent of the operator to be known, which can be very difficult and impractical. The following approach is one way to avoid this issue.

Definition 2.3. Let $A\colon \mathcal{D}(A) \subset X \to X$ be a linear operator. If $\operatorname{Re}\langle Ax, x\rangle_X \leq 0$ for all $x \in \mathcal{D}(A)$, we say that A is *dissipative*.

Even if an operator is dissipative, it may not be closed or densely defined. With this notion, we can state the Lumer–Phillips Theorem, which gives us a useful way to determine if an operator generates a contraction semigroup.

Theorem 2.1 (Lumer–Phillips Theorem)**.** Let $A\colon \mathcal{D}(A) \subset X \to X$ be a linear operator, where X is a Hilbert space. Then A is the infinitesimal generator of a contraction semi-

group $(T(t))_{t\geq 0} \subset \mathcal{L}(X)$ if and only if A is disspative and the range of $I - A$ equals X, i.e. $\mathcal{R}(I - A) = X$.

Proof. See for example [12, Theorem 6.1.7]. □

Additionally, the following theorem can be helpful.

Theorem 2.2. Let A is a linear, densely defined and closed operator on a Hilbert space X. If and only if both A and A^* are dissipative, then A is the infinitesimal generator of a contraction semigroup $(T(t))_{t\geq 0} \subset \mathcal{L}(X)$.

Proof. See [12, Theorem 6.1.8]. □

In general, not every operator has an adjoint operator. However, because A is densely defined, it has a well-defined adjoint operator.

2.5 Legendre Polynomials

The Legendre polynomials are an important case of mutually orthogonal Jacobi polynomials with respect to the standard inner product in $L^2([0,1];\mathbb{R})$. We will be using them for approximating functions defined on $[0,1]$ and finding approximate solutions to partial differential equations describing Euler–Bernoulli beams. This is possible, because we can approximate any function that is continuous on $[0,1]$ with Legendre polynomials. We cover this property in more detail later on.

There exist several equivalent definitions for the Legendre polynomials, most often defined on the interval $[-1,1]$, sometimes called the *standard Legendre polynomials*. However, we will use the following definition that defines them on $[0,1]$ instead, called the *shifted Legendre polynomials*. For $n \in \mathbb{N}$, the n-th shifted Legendre polynomial is

$$L_n(\xi) = \frac{1}{n!}\frac{d^n}{d\xi^n}(\xi^2 - \xi)^n, \qquad \xi \in [0,1]. \tag{2.8}$$

We shall derive a more useful, explicit formula.

Theorem 2.3 (Explicit Legendre Polynomial Formula)**.** An explicit formula for the n-th shifted Legendre polynomial is given by

$$L_n(\xi) = \sum_{k=0}^{n}(-1)^{n+k}\binom{n}{k}\binom{n+k}{k}\xi^k. \tag{2.9}$$

Proof. Applying the binomial theorem to $(\xi^2 - \xi)^n$ we obtain

$$(\xi^2 - \xi)^n = (-1)^n\xi^n(1-\xi)^n = (-1)^n\xi^n\sum_{k=0}^{n}\binom{n}{k}(-\xi)^k = \sum_{k=0}^{n}(-1)^{n+k}\binom{n}{k}\xi^{n+k}.$$

Differentiating the last expression n times yields

$$\begin{aligned}
&\sum_{k=0}^{n}(-1)^{n+k}\binom{n}{k}(n+k)(n+k-1)\cdots(k+2)(k+1)\xi^k \\
=&\sum_{k=0}^{n}(-1)^{n+k}\binom{n}{k}\frac{(n+k)(n+k-1)\cdots(k+2)(k+1)k!}{k!}\xi^k \\
=&\sum_{k=0}^{n}(-1)^{n+k}\binom{n}{k}\frac{(n+k)!}{k!}\xi^k.
\end{aligned}$$

Substituting this in the definition, we get

$$\begin{aligned}
L_n(\xi) &= \frac{1}{n!}\sum_{k=0}^{n}(-1)^{n+k}\binom{n}{k}\frac{(n+k)!}{k!}\xi^k \\
&= \sum_{k=0}^{n}(-1)^{n+k}\binom{n}{k}\frac{(n+k)!}{k!\,n!}\xi^k \\
&= \sum_{k=0}^{n}(-1)^{n+k}\binom{n}{k}\frac{(n+k)!}{k!\,\big((n+k)-k\big)!}\xi^k \\
&= \sum_{k=0}^{n}(-1)^{n+k}\binom{n}{k}\binom{n+k}{k}\xi^k,
\end{aligned}$$

completing the proof. □

The explicit formulation is particularly useful, as we immediately see that the coefficient of ξ^n in the n-th Legendre polynomial is $(-1)^{n+k}\binom{n}{k}\binom{n+k}{k}$. This makes computation of Legendre polynomials simple using programming languages like MATLAB, where we often represent polynomials as coefficient vectors for numerical computations.

The standard Legendre polynomials P_n defined on $[-1,1]$ can be defined as the coefficients of the power series [1, Theorem 7.2]

$$\sum_{n=0}^{\infty}P_n(\xi)s^n = \frac{1}{\sqrt{1-2\xi s+s^2}}, \qquad |s|<1. \tag{2.10}$$

We call the right hand side the *generating function* of Legendre polynomials. The shifted and standard Legendre polynomials are linked via the relation $L_n(\xi) = P_n(2\xi-1)$, where $\xi \in [0,1]$. The version for standard Legendre polynomials of (2.8) and the generating function form in (2.10) can be shown to be equivalent, see for example [4, Chapter 4] or [11, Theorem 7.10].

Theorem 2.4 (Properties of Legendre Polynomials)**.** For a shifted Legendre polynomial L_n, the following properties hold:

(i) L_n is a polynomial of degree n

(ii) $L_n(1) = 1$ and $L_n(0) = (-1)^n$

(iii) $\frac{dL_n}{d\xi}(1) = n(n+1)$ and $\frac{dL_n}{d\xi}(0) = (-1)^{n-1}n(n+1)$

(iv) $\langle L_m, L_n \rangle_{L^2} = \int_0^1 L_m(\xi)L_n(\xi)\,d\xi = \frac{1}{2n+1}\delta_{mn}$.

Proof. The first property follows directly from the definition. For proving the other properties, we apply the relation $L_n(\xi) = P_n(2\xi - 1)$. For the second property, we substitute $\xi = 1$, which yields

$$\sum_{n=0}^{\infty} L_n(1)s^n = \frac{1}{1-s}, \qquad |s| < 1.$$

The right hand side is equal to the geometric series $\sum_{n=0}^{\infty} s^n$. We have

$$\sum_{n=0}^{\infty} \big(L_n(1) - 1\big)s^n = 0, \qquad |s| < 1,$$

from which we obtain $L_n(1) = 1$. Similarly, substituting $\xi = 0$, we get

$$\sum_{n=0}^{\infty} L_n(0)s^n = \frac{1}{1+s}, \qquad |s| < 1,$$

which is equal to the geometric series $\sum_{n=0}^{\infty}(-s)^n = \sum_{n=0}^{\infty}(-1)^n s^n$. With similar reasoning, we obtain $L_n(0) = (-1)^n$. For the third property, we begin with noticing that $\frac{dL_n}{d\xi}(\xi) = 2\frac{dP_n}{d\xi}(2\xi - 1)$. Differentiating both sides of (2.10) with respect to ξ, we get

$$\sum_{n=0}^{\infty} \frac{dL_n}{d\xi}(\xi)s^n = \frac{2s}{\big(1 - (4\xi - 2)s + s^2\big)^{3/2}}, \qquad |s| < 1. \tag{2.11}$$

After differentiating the geometric series $\sum_{n=0}^{\infty} s^n$ and $\sum_{n=0}^{\infty}(-s)^n$ twice, we obtain the identities

$$\sum_{n=0}^{\infty} n(n+1)s^n = \frac{2s}{(1-s)^3} \qquad \text{and} \qquad \sum_{n=0}^{\infty}(-1)^{n-1}n(n+1)s^n = \frac{2s}{(1+s)^3}.$$

Substituting $\xi = 1$ and $\xi = 0$ in (2.11), we see that

$$\sum_{n=0}^{\infty} \frac{dL_n}{d\xi}(1)s^n = \sum_{n=0}^{\infty} n(n+1)s^n \qquad \text{and} \qquad \sum_{n=0}^{\infty} \frac{dL_n}{d\xi}(0)s^n = \sum_{n=0}^{\infty}(-1)^{n-1}n(n+1)s^n,$$

from which we obtain $\frac{dL_n}{d\xi}(1) = n(n+1)$ and $\frac{dL_n}{d\xi}(0) = (-1)^{n-1}n(n+1)$. For the fourth property, we first take

$$\int_{-1}^{1} P_m(x)P_n(x)\,dx = \frac{2}{2n+1}\delta_{mn},$$

which is obtained by combining formulas (4.3.2) and (4.6.6) in [4]. Making the substitution

$x = 2\xi - 1$, we get

$$\begin{aligned} & 2\int_0^1 P_m(2\xi-1)P_n(2\xi-1)\,d\xi = \frac{2}{2n+1}\delta_{mn} \\ \Leftrightarrow \quad & \int_0^1 L_m(\xi)L_n(\xi)\,d\xi = \frac{1}{2n+1}\delta_{mn} \\ \Leftrightarrow \quad & \langle L_m, L_n\rangle_{L^2} = \frac{1}{2n+1}\delta_{mn}. \end{aligned}$$

This completes the proof. □

The last property means the Legendre polynomials are mutually orthogonal with respect to the standard inner product in L^2.

Example 2.1. Let us compute and graph the first six Legendre polynomials. We get

$$\begin{aligned} L_0(\xi) &= \sum_{k=0}^{0}(-1)^k\binom{0}{k}\binom{k}{k}\xi^k = (-1)^0\binom{0}{0}\binom{0}{0}\xi^0 = 1 \\ L_1(\xi) &= \sum_{k=0}^{1}(-1)^{1+k}\binom{1}{k}\binom{1+k}{k}\xi^k = (-1)^1\cdot 1\cdot 1\cdot\xi^0 + (-1)^2\cdot 1\cdot 2\cdot\xi^1 = 2\xi - 1 \\ L_2(\xi) &= \sum_{k=0}^{2}(-1)^{2+k}\binom{2}{k}\binom{2+k}{k}\xi^k = 6\xi^2 - 6\xi + 1 \\ L_3(\xi) &= \sum_{k=0}^{3}(-1)^{3+k}\binom{3}{k}\binom{3+k}{k}\xi^k = 20\xi^3 - 30\xi^2 + 12\xi - 1 \\ L_4(\xi) &= \sum_{k=0}^{4}(-1)^{4+k}\binom{4}{k}\binom{4+k}{k}\xi^k = 70\xi^4 - 140\xi^3 + 90\xi^2 - 20\xi + 1 \\ L_5(\xi) &= \sum_{k=0}^{5}(-1)^{5+k}\binom{5}{k}\binom{5+k}{k}\xi^k = 252\xi^5 - 630\xi^4 + 560\xi^3 - 210\xi^2 + 30\xi - 1. \end{aligned}$$

We see that the coefficients, while integers, grow quickly in magnitude. The first six Legendre polynomials are shown in figure 2.1.

For $0 \le k \le n$, the binomial coefficient $\binom{n}{k}$ attains its largest value at $k = \lfloor \frac{n}{2} \rfloor$ and $k = \lceil \frac{n}{2} \rceil$ for a fixed n. Thus we can approximate the magnitude of the coefficients of the n-th Legendre polynomial:

$$\binom{n}{k}\binom{n+k}{k} \le \binom{n}{\lfloor \frac{n}{2} \rfloor}\binom{n+k}{\lfloor \frac{n+k}{2} \rfloor} \le \binom{n}{\lfloor \frac{n}{2} \rfloor}\binom{2n}{\lfloor \frac{2n}{2} \rfloor} \le \binom{n}{\frac{n}{2}}\binom{2n}{n}, \tag{2.12}$$

where we allow any positive numbers in the binomial coefficient. Values for non-integer inputs can be computed using the gamma function, for example. We have an asymptotic

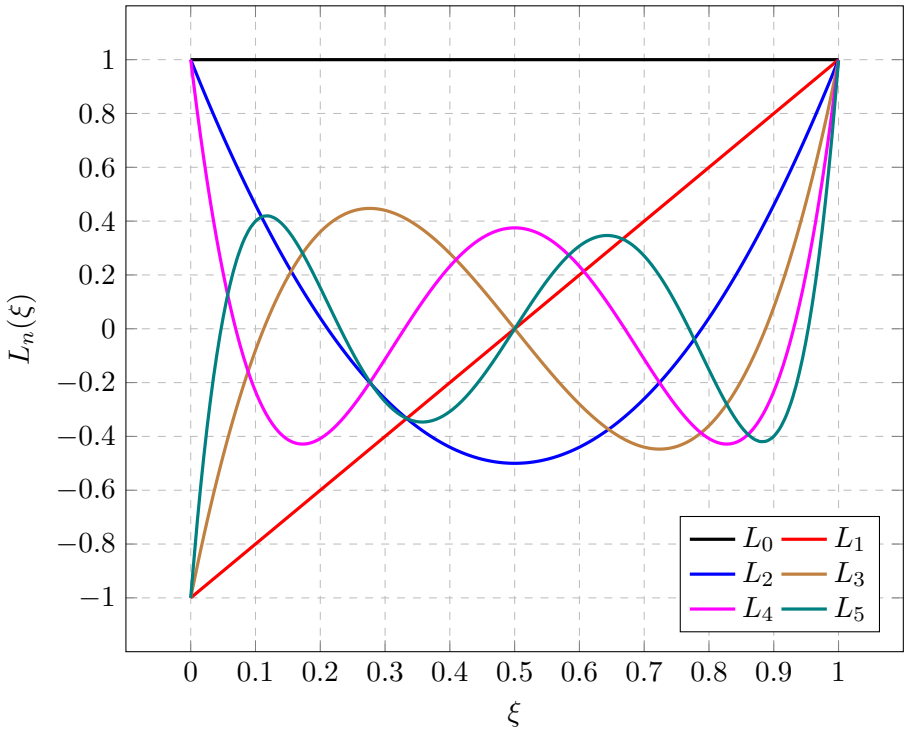

Figure 2.1. *The first six Legendre polynomials.*

approximation $\binom{2m}{m} \sim \frac{2^{2m}}{\sqrt{\pi m}}$ for large m, so from (2.12) we get

$$\binom{n}{k}\binom{n+k}{k} \leq \binom{n}{\frac{n}{2}}\binom{2n}{n} \sim \frac{2^n}{\sqrt{\frac{\pi n}{2}}}\frac{2^{2n}}{\sqrt{\pi n}} = \frac{1}{\pi n}2^{3n+\frac{1}{2}} \tag{2.13}$$

for an approximate upper bound for the magnitude of the coefficients.

Lemma 2.5. For standard Legendre polynomials, we have the recurrence relation

$$\frac{dP_{n+1}}{d\xi}(\xi) - \frac{dP_{n-1}}{d\xi}(\xi) = (2n+1)P_n(\xi), \quad n \geq 1. \tag{2.14}$$

Proof. See for example [11, Theorem 7.5]. □

Lemma 2.6. For $n \geq 1$, we have the derivative sum formula

$$\frac{dL_n}{d\xi}(\xi) = 2\sum_{\substack{k=0 \\ k+n \text{ odd}}}^{n-1}(2k+1)L_k(\xi), \quad n \geq 1. \tag{2.15}$$

Proof. Applying the shift to Lemma 2.5, we obtain

$$\frac{dL_{k+1}}{d\xi}(\xi) - \frac{dL_{k-1}}{d\xi}(\xi) = 2(2k+1)L_n(\xi), \quad k \geq 1.$$

First we assume that n is odd. Taking the sum over odd $k+n$ from $k=0$ to $k=n-1$

yields

$$\begin{aligned}
2\sum_{\substack{k=0\\ k+n \text{ odd}}}^{n-1}(2k+1)L_k(\xi) &= \sum_{\substack{k=0\\ k+n \text{ odd}}}^{n-1}\left(\frac{dL_{k+1}}{d\xi}(\xi) - \frac{dL_{k-1}}{d\xi}(\xi)\right) \\
&= \frac{dL_1}{d\xi}(\xi) - \frac{dL_{-1}}{d\xi}(\xi) + \frac{dL_3}{d\xi}(\xi) - \frac{dL_1}{d\xi}(\xi) + \frac{dL_5}{d\xi}(\xi) - \frac{dL_3}{d\xi}(\xi) \\
&\quad + \ldots + \frac{dL_{n-2}}{d\xi}(\xi) - \frac{dL_{n-4}}{d\xi}(\xi) + \frac{dL_n}{d\xi}(\xi) - \frac{dL_{n-2}}{d\xi}(\xi) \\
&= \frac{dL_n}{d\xi}(\xi),
\end{aligned}$$

where we used the convention $L_{-1}(\xi) = 0$. The case where n is even can be proven with very similar steps. □

We will derive two useful identities involving derivatives of Legendre polynomials.

Theorem 2.7. For shifted Legendre polynomials L_m and L_n, we have

$$\left\langle \frac{dL_m}{d\xi}, \frac{dL_n}{d\xi} \right\rangle_{L^2} = \begin{cases} 2(\min(m,n))^2 + 2\min(m,n), & \text{if } m+n \text{ is even} \\ 0, & \text{else} \end{cases} \tag{2.16}$$

$$\left\langle L_m, \frac{d^2L_n}{d\xi^2} \right\rangle_{L^2} = \begin{cases} 2(n-m)(m+n+1), & \text{if } n = m+2, m+4, m+6, \ldots \\ 0, & \text{else.} \end{cases} \tag{2.17}$$

Proof. First we compute

$$\begin{aligned}
\left\langle \frac{dL_m}{d\xi}, \frac{dL_n}{d\xi} \right\rangle_{L^2} &= \left\langle 2\sum_{\substack{j=0\\ j+m \text{ odd}}}^{m-1}(2j+1)L_j(\xi), \quad 2\sum_{\substack{k=0\\ k+n \text{ odd}}}^{n-1}(2k+1)L_k(\xi) \right\rangle_{L^2} \\
&= 4\sum_{\substack{j=0\\ j+m \text{ odd}}}^{m-1}\sum_{\substack{k=0\\ k+n \text{ odd}}}^{n-1}(2j+1)(2k+1)\langle L_j, L_k\rangle_{L^2} \\
&= 4\sum_{\substack{j=0\\ j+m \text{ odd}}}^{m-1}\sum_{\substack{k=0\\ k+n \text{ odd}}}^{n-1}(2j+1)(2k+1)\frac{1}{2k+1}\delta_{jk} \\
&= 4\sum_{\substack{j=0\\ j+m \text{ odd}}}^{m-1}\sum_{\substack{k=0\\ k+n \text{ odd}}}^{n-1}(2j+1)\delta_{jk}.
\end{aligned}$$

Because of the term δ_{jk}, the remaining sum will only contain terms with $j = k$. This also means whichever of m and n is smaller determines the upper bound of the sum. With all

this in mind, we can write

$$\left\langle \frac{dL_m}{d\xi}, \frac{dL_n}{d\xi} \right\rangle_{L^2} = 4 \sum_{\substack{j=0 \\ j+m \text{ odd} \\ j+n \text{ odd}}}^{\min(m,n)-1} (2j+1).$$

We immediately see that m and n must have the same parity for the expression to be non-zero. We study the cases when m and n are even and odd separately. First we assume that m and n are even. Furthermore, because the inner product is commutative, we may assume that $m \leq n$. We have

$$\sum_{\substack{j=0 \\ j+m \text{ odd} \\ j+n \text{ odd}}}^{\min(m,n)-1} (2j+1) = \sum_{\substack{j=0 \\ j \text{ odd}}}^{m-1} (2j+1) = \sum_{l=1}^{\frac{m}{2}} (2(2l-1)+1) = \sum_{l=1}^{\frac{m}{2}} (4l-1) = \frac{m^2}{2} + \frac{m}{2}.$$

For odd m and n, we proceed similarly. Again, we may assume that $m \leq n$. Thus

$$\sum_{\substack{j=0 \\ j+m \text{ odd} \\ j+n \text{ odd}}}^{\min(m,n)-1} (2j+1) = \sum_{\substack{j=0 \\ j \text{ even}}}^{m-1} (2j+1) = \sum_{l=0}^{\frac{m-1}{2}} (2(2l)+1) = \sum_{l=0}^{\frac{m-1}{2}} (4l+1) = \frac{m^2}{2} + \frac{m}{2}.$$

Conveniently, the result is the same in both cases. We can now combine these into a single result:

$$\left\langle \frac{dL_m}{d\xi}, \frac{dL_n}{d\xi} \right\rangle_{L^2} = \begin{cases} 2(\min(m,n))^2 + 2\min(m,n), & \text{if } m+n \text{ is even} \\ 0, & \text{else.} \end{cases}$$

For the second identity, we compute

$$\begin{aligned} \left\langle L_m, \frac{d^2 L_n}{d\xi^2} \right\rangle_{L^2} &= \left[L_m(\xi) \frac{dL_n}{d\xi}(\xi) \right]_0^1 - \int_0^1 \frac{dL_m}{d\xi}(\xi) \frac{dL_n}{d\xi}(\xi)\, d\xi \\ &= L_m(1) \frac{dL_n}{d\xi}(1) - L_m(0) \frac{dL_n}{d\xi}(0) - \left\langle \frac{dL_m}{d\xi}, \frac{dL_n}{d\xi} \right\rangle_{L^2} \\ &= 1 \cdot n(n+1) - (-1)^m (-1)^{n+1} n(n+1) - \left\langle \frac{dL_m}{d\xi}, \frac{dL_n}{d\xi} \right\rangle_{L^2} \\ &= \left(1 - (-1)^{m+n+1}\right) n(n+1) - \left\langle \frac{dL_m}{d\xi}, \frac{dL_n}{d\xi} \right\rangle_{L^2}. \end{aligned}$$

We see that if m and n are of different parity, thus $m+n+1$ being even, the whole expression equals zero. On the other hand, if m and n are of the same parity, $m+n+1$ is odd and we have

$$\left\langle L_m, \frac{d^2 L_n}{d\xi^2} \right\rangle_{L^2} = 2n^2 + 2n - 2(\min(m,n))^2 - 2\min(m,n).$$

If $\min(m,n) = n$, the expression equals zero. This leaves us with $\min(m,n) = m$, in which case we get

$$2n^2 + 2n - 2(\min(m,n))^2 - 2\min(m,n) = 2n^2 + 2n - 2m^2 - 2m = 2(n-m)(m+n+1).$$

Again, we combine all these into a single result, namely

$$\left\langle L_m, \frac{d^2 L_n}{d\xi^2} \right\rangle_{L^2} = \begin{cases} 2(n-m)(m+n+1), & \text{if } m < n \text{ and } m+n \text{ is even} \\ 0, & \text{else} \end{cases}$$

$$= \begin{cases} 2(n-m)(m+n+1), & \text{if } n = m+2, m+4, m+6, \dots \\ 0, & \text{else.} \end{cases}$$

This completes the proof. □

In addition to being mutually orthogonal, Legendre polynomials are excellent for approximation purposes. As polynomials with integer coefficients, they are easy to compute numerically and to work with. Assume $f\colon [0,1] \to \mathbb{R}$ is a continuous function on the whole interval $[0,1]$ and has a continuous derivative on $[0,1]$, i.e. $f \in C^1([0,1];\mathbb{R})$. Then there exists a *Fourier–Legendre series expansion* [11, Theorem 7.11] such that

$$f(\xi) = \sum_{n=0}^{\infty} a_n L_n(\xi), \quad a_n \in \mathbb{R}. \tag{2.18}$$

The Fourier–Legendre series converges uniformly for $\xi \in [0,1]$. We can find the coefficients a_n with the following approach. Because the series is convergent, we take the inner product with L_m of both sides of (2.18). We get

$$\langle f, L_m \rangle_{L^2} = \left\langle \sum_{n=0}^{\infty} a_n L_n, L_m \right\rangle_{L^2} = \sum_{n=0}^{\infty} a_n \langle L_n, L_m \rangle_{L^2} = \sum_{n=0}^{\infty} \frac{a_n}{2n+1} \delta_{mn} = \frac{a_m}{2m+1}, \tag{2.19}$$

and the formula for the n-th coefficient becomes

$$a_n = (2n+1)\langle f, L_n \rangle_{L^2}. \tag{2.20}$$

By truncating (2.18), we obtain a polynomial approximation of f on $[0,1]$. Because the series expansion converges uniformly, for any $\epsilon > 0$ we can find $N \in \mathbb{N}$ such that $\sup \left| f(\xi) - \sum_{n=0}^{N} a_n L_n(\xi) \right| < \epsilon$, where $\xi \in [0,1]$.

3 EULER–BERNOULLI BEAM THEORY

The goal of this chapter is to cover the basic ideas related to the Euler–Bernoulli beam theory. Later in this work, we are exclusively interested in the dynamic beam equation, describing the behaviour of a beam as a partial differential equation. For completeness, we first study the static beam equation.

3.1 Static Beam Equation

Consider a structure that is much larger in one dimension than the other two, for example a thin rod made of metal. We can model this as a line segment $\Omega = [L_1, L_2] \subset \mathbb{R}$. Usually we have $\Omega = [0, 1]$ or $\Omega = [-1, 1]$.

Figure 3.1. *Mathematical beam Ω in the ξw-plane.*

With respect to the above figure, we are only interested in loads perpendicular to the beam's axis, i.e. loads in the w-direction.

Let us denote the deflection curve of a beam with $w\colon \Omega \to \mathbb{R}$. In figure 3.1, $\Omega = [0, 1]$ and the deflection is zero everywhere, i.e. $w \equiv 0$. The deflection curve determines the shape of the beam. We are modelling a continuous structure, so we assume w to be at least continuous. More precise requirements for w are studied later.

Assume w is continuously differentiable four times, i.e. $w \in C^4(\Omega; \mathbb{R})$ and $\xi \in \Omega$. The general one-dimensional Euler–Bernoulli equation for a static beam is [7, pp. 480–484]

$$\frac{d^2}{d\xi^2}\left(E(\xi)I(\xi)\frac{d^2w}{d\xi^2}(\xi)\right) = q(\xi), \tag{3.1}$$

where E is the *elastic modulus* of the beam, I is the *second moment of area* of the beam's cross section, and q denotes the net force acting on the beam. The product EI is often called the *flexural rigidity*. In general, both parameters E and I vary by location. Examples of this include a beam with varying thickness or a beam of inhomogeneous

material. In case of a beam made of homogeneous material that is of uniform thickness, E and I are constant and (3.1) simplifies to

$$EI\frac{d^4w}{d\xi^4}(\xi) = q(\xi), \tag{3.2}$$

which is solvable by standard methods for ordinary differential equations. The Euler–Bernoulli beam model is limited to cases where the deflection and curvature of the beam remain small enough relative to the length of the beam. We will not study inhomogeneous beams in this work, but for the interested reader, they are covered in detail in [6, Chapter 7].

3.2 Boundary Conditions for Beams

In order to obtain a unique solution for (3.2), which is a fourth-order ordinary differential equation, four boundary conditions are needed. The boundary conditions are determined by how the beam is supported at the endpoints. Here we study three basic cases of different endpoint supports for beams. First, we define two concepts needed to understand the boundary conditions.

Definition 3.1 (The Bending Moment and the Shear Force)**.** Let $w\colon \Omega \to \mathbb{R}$ denote the deflection of a beam and assume $w \in C^4(\Omega;\mathbb{R})$. The *bending moment* of the beam is

$$M(\xi) = -E(\xi)I(\xi)\frac{d^2w}{d\xi^2}(\xi), \tag{3.3}$$

and the *shear force* is

$$Q(\xi) = -\frac{d}{d\xi}\left(E(\xi)I(\xi)\frac{d^2w}{d\xi^2}(\xi)\right). \tag{3.4}$$

If E and I are constant, the formulation of the shear force simplifies to

$$Q(\xi) = -EI\frac{d^3w}{d\xi^3}(\xi). \tag{3.5}$$

In case there is no support at an endpoint, the endpoint is called a *free end*. This is because there is no external forces acting on the endpoint. This corresponds to both the bending moment and the shear force being equal to zero, from which we obtain

$$\begin{cases} \dfrac{d^2w}{d^2\xi}(l) = 0 & \text{(no bending moment)} \\ \dfrac{d^3w}{d^3\xi}(l) = 0, & \text{(no shear force)} \end{cases} \tag{3.6}$$

where l is the endpoint in question. If the beam is pinned at an endpoint, it is called a *simply supported end*. This type of support allows the beam to rotate freely but staying fixed in place otherwise, which means the deflection must stay constant at the endpoint

and the bending moment must equal zero. From this we obtain

$$\begin{cases} w(l) = c & \text{(fixed deflection)} \\ \dfrac{d^2w}{d^2\xi}(l) = 0, & \text{(no bending moment)} \end{cases} \tag{3.7}$$

where c is a constant. If we have one simply supported end, often in applications we fix the coordinate system so that $c = 0$. The third type of endpoint support we cover is *clamping*, which fixes both the deflection and the slope of the beam at the endpoint $\xi = l$. This yields the following boundary conditions:

$$\begin{cases} w(l) = c_1 & \text{(fixed deflection)} \\ \dfrac{dw}{d\xi}(l) = c_2, & \text{(fixed slope)} \end{cases} \tag{3.8}$$

where c_1 and c_2 are constants. In applications, we usually have $c_1 = c_2 = 0$, which corresponds to a horizontally clamped beam.

3.3 Types of Beams and Examples

In this section, we study two standard examples of static beams; the *simply supported beam* and the *cantilevered beam* through two introductory examples by solving (3.2) for the deflection curve $w = w(\xi)$.

Example 3.1 (A Simply Supported Beam)**.** Let $\Omega = [0, 1]$ and $EI = 100$. We have a beam which is simply supported at $\xi = 0$ and $\xi = 1$ with $q \equiv -1$ (opposite direction to the w-axis). Our boundary conditions are those described in (3.7) for both ends with $c = 0$. Integrating (3.2) four times gives

$$w(\xi) = -\frac{1}{100}\left(\frac{1}{24}\xi^4 + \frac{1}{6}c_3\xi^3 + \frac{1}{2}c_2\xi^2 + c_1\xi + c_0\right), \tag{3.9}$$

where c_i are constants determined by the boundary conditions. Applying the boundary conditions $w(0) = w(1) = \frac{d^2w}{d\xi^2}(0) = \frac{d^2w}{d\xi^2}(1) = 0$, we get $c_0 = 0$, $c_1 = 1/24$, $c_2 = 0$ and $c_3 = -1/2$. The deflection curve of our beam is

$$w(\xi) = \frac{1}{2400}\big(-\xi^4 + 2\xi^3 - \xi\big). \tag{3.10}$$

The solution is a polynomial, so it has infinitely many continuous derivatives and thus $w \in C^4([0, 1]; \mathbb{R})$. The solution is shown in figure 3.2.

Example 3.2 (A Cantilevered Beam)**.** Let $\Omega = [0, 1]$ and $EI = 100$. This time, we have a cantilevered beam that is horizontally clamped at $\xi = 0$ and its free end is at $\xi = 1$. Let our load distribution be $q(\xi) = 4\xi(\xi - 1)$. Substituting these into (3.2) and integrating four

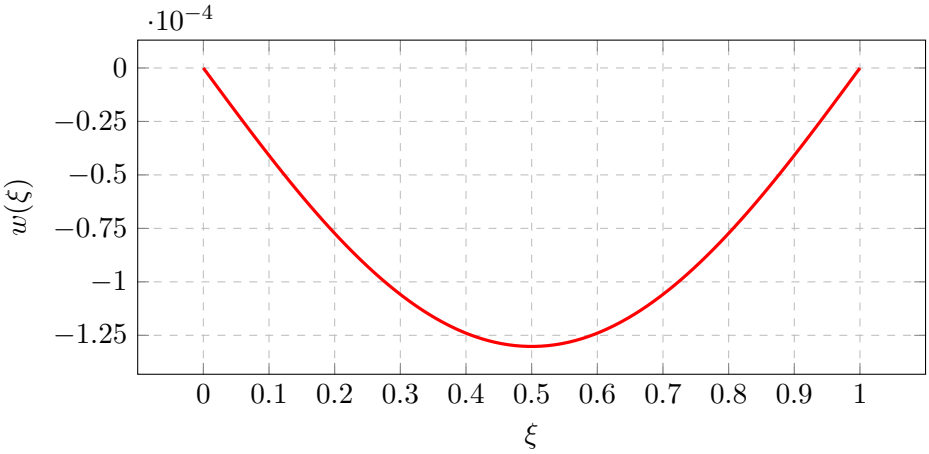

Figure 3.2. *The solution to example 3.1.*

times we get

$$w(\xi) = \frac{1}{100}\left(\frac{1}{90}\xi^6 - \frac{1}{30}\xi^5 + \frac{1}{6}c_3\xi^3 + \frac{1}{2}c_2\xi^2 + c_1\xi + c_0\right). \tag{3.11}$$

The left end of the beam is clamped and the right end is free, thus our boundary conditions are $w(0) = \frac{dw}{d\xi}(0) = 0$ and $\frac{d^2w}{d\xi^2}(1) = \frac{d^3w}{d\xi^3}(1) = 0$, respectively. Applying the boundary conditions we get $c_0 = c_1 = 0$, $c_2 = -1/3$ and $c_3 = 2/3$. Finally, our solution is

$$w(\xi) = \frac{1}{9000}\left(\xi^6 - 3\xi^5 + 10\xi^3 - 15\xi^2\right). \tag{3.12}$$

Again, as a polynomial, the solution is in $C^4([0,1];\mathbb{R})$. The solution is shown in figure 3.3.

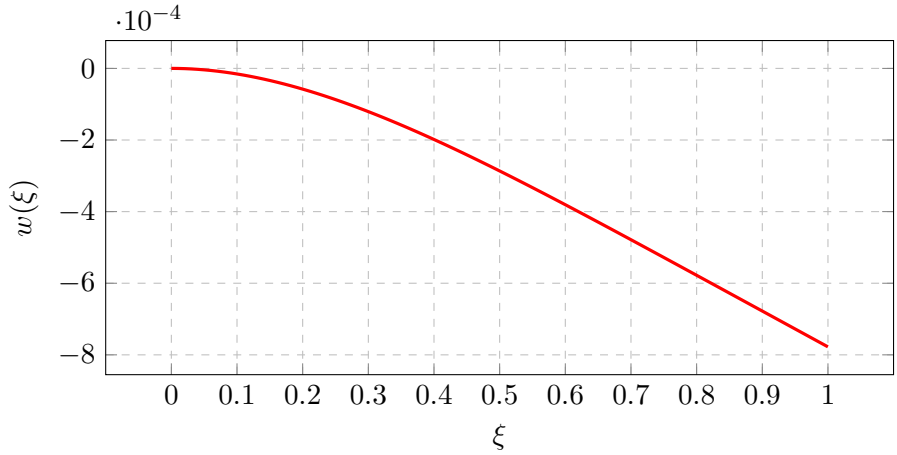

Figure 3.3. *The solution to example 3.2.*

Problems in statics involving beam structures can in general be much more complicated than the two examples provided. For example, a beam could be supported at several points or the net force could be a complicated piecewise function, possibly containing discontinuities. Additionally, many real life problems involve point forces and torques which do not behave as nicely as the simple loads in our examples. We will not go further into studying static beams in this work.

3.4 Dynamic Beam Equation

In this section, we cover the basics of time-dependent Euler–Bernoulli beams. From this point on, we will use $\Omega = [0, 1]$ as our spatial domain. We may do this without loss of generality, since any domain of the form $\Omega = [L_1, L_2]$ can be mapped one-to-one to $[0, 1]$ with the transform $\xi \mapsto \frac{1}{L_2 - L_1}(\xi - L_1)$.

The general dynamic Euler–Bernoulli beam equation with viscous damping is

$$\frac{\partial^2}{\partial \xi^2}\left(E(\xi)I(\xi)\frac{\partial^2 w}{\partial \xi^2}(\xi, t)\right) = -\mu(\xi)\frac{\partial^2 w}{\partial t^2}(\xi, t) - \gamma\frac{\partial w}{\partial t}(\xi, t) + q(\xi), \qquad 0 < \xi < 1, \quad t > 0, \tag{3.13}$$

where μ represents mass per unit length and $\gamma > 0$ is the viscous damping coefficient. The other parameters are the same as before. If we have a homogeneous beam and no external forces acting on the beam, E, I and μ are constants, $q \equiv 0$ and the equation becomes

$$\frac{\partial^2 w}{\partial t^2}(\xi, t) + \frac{EI}{\rho a}\frac{\partial^4 w}{\partial \xi^4}(\xi, t) + \frac{\gamma}{\rho a}\frac{\partial w}{\partial t}(\xi, t) = 0, \qquad 0 < \xi < 1, \quad t > 0, \tag{3.14}$$

where a is the cross-sectional area of the beam and ρ is its mass density, thus $\mu = \rho a$. In order for the partial differential equation to have a unique solution, it needs four boundary conditions, two at $\xi = 0$ and two at $\xi = 1$, and two initial conditions at $t = 0$. This is because the equation is fourth-order in ξ and second-order in t. As is the case with most partial differential equations, there is no general analytic solution for any of the equations describing a time-evolving Euler–Bernoulli beam. In the following chapter, we implement a numerical method for solving (3.14) using the spectral Galerkin method with Legendre polynomials.

Generally, in the introductory examples of partial differential equations, only boundary conditions independent of time are considered. However, in this work we need time-dependent boundary conditions, which we use as a way to have an input to the system. Boundary control inputs are usually denoted by $u = u(t),\ t > 0$. For generality, we address the four boundary conditions for (3.14) as functions of time. This includes static boundary conditions as constant functions. We can express the general boundary conditions as

$$\frac{\partial^m w}{\partial \xi^m}(0, t) = u_1(t), \quad \frac{\partial^n w}{\partial \xi^n}(0, t) = u_2(t), \quad \frac{\partial^p w}{\partial \xi^p}(1, t) = u_3(t), \quad \frac{\partial^q w}{\partial \xi^q}(1, t) = u_4(t), \tag{3.15}$$

where $m, n, p, q \in \{0, 1, 2, 3\}$ with $m \neq n$ and $p \neq q$. Suppose the initial conditions for (3.14) are

$$w(\xi, 0) = w_0(\xi) \qquad \text{and} \qquad \frac{\partial w}{\partial t}(\xi, 0) = w_1(\xi). \tag{3.16}$$

These describe the deflection profile and the velocity of the beam at $t = 0$. However, in order to have a ”well-behaving system”, we need to consider the properties of the

boundary input functions. For $k = 1, 2, 3, 4$, we assume u_k satisfies the following:

- u_k is twice continuously differentiable on $[0, \infty)$, i.e. $u_k \in C^2([0, \infty); \mathbb{R})$
- $u_k(0)$ is such that w_0 and w_1 satisfy (3.15) at $t = 0$.

The first requirement guarantees that our boundary control input behaves smoothly enough without any abrupt changes. The second requirement guarantees that the boundary values change continuously from the initial state.

3.5 Solution via Separation of Variables

We can solve (3.14) assuming a solution of the form $w(\xi, t) = F(\xi)G(t)$, sometimes called a *separable solution*. Furthermore, we assume that all the physical parameters are constant and there are no external forces acting on the beam. Let $F \in C^4([0, 1]; \mathbb{R})$ and $G \in C^2([0, \infty); \mathbb{R})$. Substituting $w(\xi, t) = F(\xi)G(t)$ into (3.14) yields

$$\begin{aligned} & F(\xi)\frac{d^2G}{dt^2}(t) + \frac{EI}{\rho a}\frac{d^4F}{d\xi^4}(\xi)G(t) + \frac{\gamma}{\rho a}F(\xi)\frac{dG}{dt}(t) = 0 \\ \Leftrightarrow \quad & \frac{EI}{\rho a}\frac{1}{F(\xi)}\frac{d^4F}{d\xi^4}(\xi) = -\frac{1}{G(t)}\left(\frac{d^2G}{dt^2}(t) + \frac{\gamma}{\rho a}\frac{dG}{dt}(t)\right). \end{aligned} \tag{3.17}$$

Because the left hand side of (3.17) depends only on ξ and the right hand side only on t, they must equal the same constant $\lambda \in \mathbb{R}$. We get two equations:

$$\begin{cases} \lambda F(\xi) = \dfrac{EI}{\rho a}\dfrac{d^4}{d\xi^4}F(\xi) \\ \lambda G(t) = -\dfrac{d^2}{dt^2}G(t) - \dfrac{\gamma}{\rho a}\dfrac{d}{dt}G(t), \end{cases} \tag{3.18}$$

which are ordinary differential equations in ξ and t, respectively. The first equation has a general solution

$$F(\xi) = C_1 \sin(\kappa\xi) + C_2 \cos(\kappa\xi) + C_3 \sinh(\kappa\xi) + C_4 \cosh(\kappa\xi), \tag{3.19}$$

where $\kappa = \sqrt[4]{\frac{\rho a \lambda}{EI}}$. Constants C_j are determined by four boundary conditions. Likewise, we can solve the second equation to get

$$G(t) = e^{-\alpha t}\Big(D_1 e^{-\beta t} + D_2 e^{\beta t}\Big), \tag{3.20}$$

where

$$\alpha = \frac{\gamma}{2\rho a} \qquad \text{and} \qquad \beta = \sqrt{\Big(\frac{\gamma}{2\rho a}\Big)^2 - \lambda} = \sqrt{\alpha^2 - \lambda}. \tag{3.21}$$

We see that $\alpha > 0$, but generally $\beta \in \mathbb{C}$. Constants D_1 and D_2 are determined by two initial conditions. In order to have a classical solution, our initial conditions must be of the

form

$$\begin{cases} w_0(\xi) = w(\xi, 0) = F(\xi)G(0) = (D_1 + D_2)F(\xi) \\ w_1(\xi) = \dfrac{\partial w}{\partial t}(\xi, 0) = F(\xi)\dfrac{dG}{dt}(0) = \big((-\alpha - \beta)D_1 + (-\alpha + \beta)D_2\big)F(\xi), \end{cases} \tag{3.22}$$

where $D_1, D_2 \in \mathbb{R}$ In case where $\lambda > \alpha^2$, we obtain a simpler form without complex numbers, using the formula $e^{ix} = \cos x + i \sin x$:

$$G(t) = e^{-\alpha t}\Big(E_1 \sin\big(\tilde{\beta}t\big) + E_2 \cos\big(\tilde{\beta}t\big)\Big), \tag{3.23}$$

where α is the same as before and $\tilde{\beta} = \sqrt{\lambda - \alpha^2}$.

We still need to find out what λ is in the solutions. It turns out that the boundary conditions for a beam determine a countable set $\{\lambda_n\}_{n=0}^{\infty} \subset \mathbb{R}$ for which the system (3.18) is solvable. Additionally, we assumed our solutions to be real, so in order to (3.19) be real, we must have $\lambda_n \geq 0$. Because each value $\lambda_n \in \{\lambda_n\}_{n=0}^{\infty}$ yields a solution to (3.18) and it is a system of two linear ordinary differential equations, the full solution is

$$w(\xi, t) = \sum_{n=0}^{\infty} \alpha_n F_n(\xi) G_n(t), \qquad \alpha_n \in \mathbb{R}, \tag{3.24}$$

where F_n and G_n are as in (3.19) and (3.20) for each λ_n, respectively. We study specific solutions to (3.18) in the following example.

Example 3.3 (Vibrating Modes of a Cantilevered Beam)**.** Assume a horizontally cantilevered beam with the fixed end at $\xi = 0$ and the free end at $\xi = 1$. Our boundary conditions are $F(0) = \frac{dF}{d\xi}(0) = 0$ and $\frac{d^2F}{d\xi^2}(1) = \frac{d^3F}{d\xi^3}(1) = 0$. Applying these to (3.19), we get

$$\begin{cases} F(0) = C_2 + C_4 = 0 \\ \dfrac{dF}{d\xi}(0) = C_1 + C_3 = 0 \\ \dfrac{d^2F}{d\xi^2}(1) = -C_1 \sin\kappa - C_2 \cos\kappa + C_3 \sinh\kappa + C_4 \cosh\kappa = 0 \\ \dfrac{d^3F}{d\xi^3}(1) = -C_1 \cos\kappa + C_2 \sin\kappa + C_3 \cosh\kappa + C_4 \sinh\kappa = 0. \end{cases} \tag{3.25}$$

Solving for $C_3 = -C_1$ and $C_4 = -C_2$ from the first two equations and substituting these into the last two we obtain

$$\begin{cases} C_1 \sin\kappa + C_2 \cos\kappa + C_1 \sinh\kappa + C_2 \cosh\kappa = 0 \\ C_1 \cos\kappa - C_2 \sin\kappa + C_1 \cosh\kappa + C_2 \sinh\kappa = 0. \end{cases} \tag{3.26}$$

Furthermore, assuming $C_1, C_2 \neq 0$, we get the relation

$$\frac{\sin\kappa + \sinh\kappa}{\cos\kappa + \cosh\kappa} = \frac{\cos\kappa + \cosh\kappa}{-\sin\kappa + \sinh\kappa}, \tag{3.27}$$

which we can simplify using the identities $\cos^2 x + \sin^2 x = 1$ and $\cosh^2 x - \sinh^2 x = 1$ to get

$$\cos\kappa\cosh\kappa + 1 = 0 \quad \Leftrightarrow \quad \cos\kappa + \frac{1}{\cosh\kappa} = 0, \tag{3.28}$$

recalling that $\cosh x \geq 1$ for all real numbers x. We define the function $h\colon [0,\infty) \to \mathbb{R}$, $h(\kappa) = \cos\kappa + 1/\cosh\kappa$ to investigate the solutions to (3.28). Note that $\cosh\kappa$ grows exponentially, so $1/\cosh\kappa \to 0$ very quickly as $\kappa \to \infty$. This means that $h(\kappa) \approx \cos\kappa$ for large κ and consequently the roots of h are approximately those of the cosine function, namely $\kappa_n \approx (n + 1/2)\pi$ for $n = 0, 1, 2, \ldots$ as we want the roots to be non-negative.

We have $C_3 = -C_1$, $C_4 = -C_2$ and from the first equation of (3.26) we can solve for C_2. Denoting

$$\Lambda_n = \frac{\sin\kappa_n + \sinh\kappa_n}{\cos\kappa_n + \cosh\kappa_n}, \tag{3.29}$$

we obtain the modes of the cantilevered beam:

$$F_n(\xi) = C_n\big(\sin(\kappa_n\xi) - \sinh(\kappa_n\xi) + \Lambda_n(\cosh(\kappa_n\xi) - \cos(\kappa_n\xi))\big), \tag{3.30}$$

where κ_n are the positive solutions to $\cos\kappa_n\cosh\kappa_n + 1 = 0$ and C_n is a constant. If we denote $\lambda = \omega^2$ with $\omega > 0$, we have $\kappa_n = \sqrt[4]{\frac{\rho a\omega_n^2}{EI}}$, from which we get

$$\omega_n = \kappa_n^2\sqrt{\frac{EI}{\rho a}} \sim (n + 1/2)^2\pi^2\sqrt{\frac{EI}{\rho a}}. \tag{3.31}$$

The values ω_n correspond to the angular frequencies of the beam modes, which we can see in the forms (3.20) and (3.23). Differently supported beams can be studied in the same vein, yielding similar formulations.

3.6 Energy Space Formulation

For constant physical parameters, we can transform (3.14) into a linear system of two first order equations in time by introducing two new variables:

$$x_1(\xi,t) \coloneqq \rho a\frac{\partial w}{\partial t}(\xi,t) \qquad \text{and} \qquad x_2(\xi,t) \coloneqq \frac{\partial^2 w}{\partial\xi^2}(\xi,t), \tag{3.32}$$

which we call the *energy variables*. The term comes from the choice of our state variables, which links the system naturally to its Hamiltonian, in our case the mechanical energy of

the beam. The mechanical energy of a beam is equal to [3, Eq. 1, Eq. 2]

$$\begin{aligned} E(t) &= E_k(t) + E_p(t) \\ &= \frac{1}{2}\rho a \int_0^1 \left(\frac{\partial w}{\partial t}(\xi,t)\right)^2 d\xi + \frac{1}{2} EI \int_0^1 \left(\frac{\partial^2 w}{\partial \xi^2}(\xi,t)\right)^2 d\xi \\ &= \frac{1}{2}\int_0^1 \frac{1}{\rho a}\big(x_1(\xi,t)\big)^2 d\xi + \frac{1}{2}\int_0^1 EI\big(x_2(\xi,t)\big)^2 d\xi \\ &= \frac{1}{2}\frac{1}{\rho a}\big\langle x_1(\cdot,t), x_1(\cdot,t)\big\rangle_{L^2} + \frac{1}{2} EI \big\langle x_2(\cdot,t), x_2(\cdot,t)\big\rangle_{L^2} \\ &= \frac{1}{2}\frac{1}{\rho a}\left\|x_1(\cdot,t)\right\|_{L^2}^2 + \frac{1}{2} EI \left\|x_2(\cdot,t)\right\|_{L^2}^2 . \end{aligned} \tag{3.33}$$

We transform (3.14) into a system of two partial differential equations that are of first order in time. We get

$$\begin{cases} \dfrac{\partial^2 w}{\partial t^2}(\xi,t) = -\dfrac{EI}{\rho a}\dfrac{\partial^4 w}{\partial \xi^4}(\xi,t) - \dfrac{\gamma}{\rho a}\dfrac{\partial w}{\partial t}(\xi,t) \\ \dfrac{\partial^3 w}{\partial \xi^2 \partial t}(\xi,t) = \dfrac{\partial^3 w}{\partial \xi^2 \partial t}(\xi,t). \end{cases} \tag{3.34}$$

Noting that

$$\frac{\partial w}{\partial t}(\xi,t) = \frac{1}{\rho a} x_1(\xi,t), \quad \frac{\partial^2 w}{\partial t^2}(\xi,t) = \frac{1}{\rho a}\frac{\partial x_1}{\partial t}(\xi,t), \quad \frac{\partial^4 w}{\partial \xi^4}(\xi,t) = \frac{\partial^2 x_2}{\partial \xi^2}(\xi,t) \quad \text{and}$$

$$\frac{\partial^3 w}{\partial \xi^2 \partial t}(\xi,t) = \frac{\partial x_2}{\partial t}(\xi,t) = \frac{1}{\rho a}\frac{\partial^2 x_1}{\partial \xi^2}(\xi,t),$$

we get

$$\begin{cases} \dfrac{\partial x_1}{\partial t}(\xi,t) = -\dfrac{\gamma}{\rho a} x_1(\xi,t) - EI\dfrac{\partial^2 x_2}{\partial \xi^2}(\xi,t) \\ \dfrac{\partial x_2}{\partial t}(\xi,t) = \dfrac{1}{\rho a}\dfrac{\partial^2 x_1}{\partial \xi^2}(\xi,t). \end{cases} \tag{3.35}$$

However, with the new variables, we also need to express the initial conditions in terms of the new variables x_1 and x_2. For the original partial differential equation, the initial conditions are $w(\xi,0) = w_0(\xi)$ and $\frac{\partial w}{\partial t}(\xi,0) = w_1(\xi)$. Additionally, we assume that $w_0 \in C^2([0,1];\mathbb{R})$. We obtain

$$\begin{cases} x_1(\xi,0) = \rho a \dfrac{\partial w}{\partial t}(\xi,0) = \rho a w_1(\xi), \\ x_2(\xi,0) = \dfrac{\partial^2 w}{\partial \xi^2}(\xi,0) = \dfrac{d^2 w_0}{d\xi^2}(\xi). \end{cases} \tag{3.36}$$

We can represent (3.35) as an abstract differential equation, namely

$$\begin{cases} \dfrac{d}{dt}x(t) = Ax(t), \qquad t > 0, \\ \quad x(0) = \begin{bmatrix} \rho a w_1 \\ \frac{d^2 w_0}{d\xi^2} \end{bmatrix}, \end{cases} \tag{3.37}$$

where

$$A = \begin{bmatrix} -\frac{\gamma}{\rho a} & -EI\frac{\partial^2}{\partial \xi^2} \\ \frac{1}{\rho a}\frac{\partial^2}{\partial \xi^2} & 0 \end{bmatrix} \qquad \text{and} \qquad x(t) = \begin{bmatrix} x_1(t) \\ x_2(t) \end{bmatrix}. \tag{3.38}$$

We dropped the spatial variable ξ from the formulation to emphasise that we are studying an abstract differential equation in time. Time-dependent boundary conditions in (3.15) can be formulated in terms of the energy variables in the following way. Let $l \in \{0, 1\}$ and u be a valid boundary input. Then we have the conversions

$$w(l,t) = u(t) \qquad \Rightarrow \qquad x_1(l,t) = \rho a \frac{du}{dt}(t) \tag{3.39}$$

$$\frac{\partial w}{\partial \xi}(l,t) = u(t) \qquad \Rightarrow \qquad \frac{\partial x_1}{\partial \xi}(l,t) = \rho a \frac{du}{dt}(t) \tag{3.40}$$

$$\frac{\partial^2 w}{\partial \xi^2}(l,t) = u(t) \qquad \Rightarrow \qquad x_2(l,t) = u(t) \tag{3.41}$$

$$\frac{\partial^3 w}{\partial \xi^3}(l,t) = u(t) \qquad \Rightarrow \qquad \frac{\partial x_2}{\partial \xi}(l,t) = u(t). \tag{3.42}$$

We see that the four boundary conditions needed to solve (3.14), two for $\xi = 0$ and two for $\xi = 1$, correspond to four boundary conditions for (3.35), two for $\xi = 0$ and two for $\xi = 1$. Because $u \in C^2([0, \infty); \mathbb{R})$, the "converted" boundary inputs for the energy variables are all (at least once) continuously differentiable. Later on in this work, we will apply boundary inputs directly to the energy variables. We assume that all such boundary input functions $\tilde{u}$ are continuously differentiable, i.e. $\tilde{u} \in C^1([0, \infty); \mathbb{R})$.

3.7 Generation of Contraction Semigroups

In this section, we study which linear combinations of homogeneous boundary conditions for the energy variables x_1, x_2 in (3.35) determine a semigroup. More specifically, we study when the operator A in (3.38) generates a contraction semigroup.

Several types of abstract differential equations can be formulated as *port-Hamiltonian systems*, which are systems expressible in the form [2, pp. 3–4]

$$\frac{\partial x}{\partial t}(\xi, t) = \sum_{k=0}^{N} P_k \frac{\partial^k (\mathcal{H}x)}{\partial \xi^k}(\xi, t), \qquad 0 < \xi < 1, \quad t > 0, \tag{3.43}$$

where $P_k \in \mathbb{C}^{d\times d}$ that satisfy the condition

$$P_k^* = (-1)^{k-1}P_k, \qquad k \geq 1. \tag{3.44}$$

We also assume that P_N is invertible. Generally, $\mathcal{H}$ denotes the *Hamiltonian density function* $\mathcal{H}\colon (0,1) \to \mathbb{C}^{d\times d}$, which is a measurable function such that for almost every $\xi \in (0,1)$ the matrix $\mathcal{H}(\xi)$ is self-adjoint and

$$m \left\|z\right\|_{\mathbb{C}^d}^2 \leq z^*\mathcal{H}(\xi)z \leq M \left\|z\right\|_{\mathbb{C}^d}^2, \qquad z \in \mathbb{C}^d \tag{3.45}$$

for some $0 < m \leq M$. If these hold, we say that $\mathcal{H}$ is *uniformly positive*.

Lemma 3.1. Let $\mathcal{H} \in \mathbb{C}^{d\times d}$ be a constant diagonal matrix with positive diagonal elements, i.e. $\mathcal{H}(\xi) = \operatorname{diag}(a_1, a_2, \ldots, a_d)$ with $a_i > 0$. Then $\mathcal{H}$ is a measurable function on $(0,1)$, $\mathcal{H}(\xi)$ is self-adjoint for $\xi \in (0,1)$ and $m \left\|z\right\|_{\mathbb{C}^d}^2 \leq z^*\mathcal{H}(\xi)z \leq M \left\|z\right\|_{\mathbb{C}^d}^2$ holds for some $0 < m \leq M$ and all $z \in \mathbb{C}^d$.

Proof. Let $z = [\,z_1\ z_2\ \cdots\ z_d\,]^{\mathsf{T}} \in \mathbb{C}^d$ and $\mathcal{H}(\xi) = \operatorname{diag}(a_1, a_2, \ldots, a_d) \in \mathbb{C}^{d\times d}$, $\xi \in (0,1)$. Furthermore, let $a_m = \min\{a_1, a_2, \ldots, a_d\}$ and $a_M = \max\{a_1, a_2, \ldots, a_d\}$. We have

$$\begin{aligned} z^*\mathcal{H}(\xi)z &= \begin{bmatrix} \bar{z}_1 & \bar{z}_2 & \cdots & \bar{z}_d \end{bmatrix} \begin{bmatrix} a_1 & & & \\ & a_2 & & \\ & & \ddots & \\ & & & a_d \end{bmatrix} \begin{bmatrix} z_1 \\ z_2 \\ \vdots \\ z_d \end{bmatrix} \\ &= a_1 z_1 \bar{z}_1 + a_2 z_2 \bar{z}_2 + \ldots + a_d z_d \bar{z}_d \\ &= a_1 \left|z_1\right|^2 + a_2 \left|z_2\right|^2 + \ldots + a_d \left|z_d\right|^2, \end{aligned}$$

which implies

$$a_m \left\|z\right\|_{\mathbb{C}^d}^2 \leq z^*\mathcal{H}(\xi)z \leq a_M \left\|z\right\|_{\mathbb{C}^d}^2.$$

Because $\mathcal{H}(\xi)$ is a real diagonal matrix, it is self-adjoint. As a constant function, $\mathcal{H}$ is measurable on $(0,1)$. This completes the proof. □

We can reformulate (3.38) as

$$\begin{aligned} \frac{d}{dt}\begin{bmatrix} x_1(t) \\ x_2(t) \end{bmatrix} &= \begin{bmatrix} 0 & -EI\frac{\partial^2}{\partial\xi^2} \\ \frac{1}{\rho a}\frac{\partial^2}{\partial\xi^2} & 0 \end{bmatrix} \begin{bmatrix} x_1(t) \\ x_2(t) \end{bmatrix} + \begin{bmatrix} -\frac{\gamma}{\rho a} & 0 \\ 0 & 0 \end{bmatrix} \begin{bmatrix} x_1(t) \\ x_2(t) \end{bmatrix} \\ &= \begin{bmatrix} 0 & -1 \\ 1 & 0 \end{bmatrix} \frac{\partial^2}{\partial\xi^2} \begin{bmatrix} \frac{1}{\rho a} & 0 \\ 0 & EI \end{bmatrix} \begin{bmatrix} x_1(t) \\ x_2(t) \end{bmatrix} + \begin{bmatrix} -\gamma & 0 \\ 0 & 0 \end{bmatrix} \begin{bmatrix} \frac{1}{\rho a} & 0 \\ 0 & EI \end{bmatrix} \begin{bmatrix} x_1(t) \\ x_2(t) \end{bmatrix}. \end{aligned} \tag{3.46}$$

This is in the standard port-Hamiltonian form with $N = 2$ and

$$P_2 = \begin{bmatrix} 0 & -1 \\ 1 & 0 \end{bmatrix}, \quad P_1 = \begin{bmatrix} 0 & 0 \\ 0 & 0 \end{bmatrix}, \quad P_0 = \begin{bmatrix} -\gamma & 0 \\ 0 & 0 \end{bmatrix}, \quad \mathcal{H} = \begin{bmatrix} \frac{1}{\rho a} & 0 \\ 0 & EI \end{bmatrix},$$

$$x(t) = \begin{bmatrix} x_1(t) \\ x_2(t) \end{bmatrix} = \begin{bmatrix} \rho a \frac{\partial w}{\partial t}(\xi, t) \\ \frac{\partial^2 w}{\partial \xi^2}(\xi, t) \end{bmatrix},$$

because $P_2 = -P_2^*$ is invertible, $P_1 = P_1^*$ and $\mathcal{H}$ satisfies the requirements of a Hamiltonian density function, based on Lemma 3.1. We collect the boundary values of $\mathcal{H}x_1$, $\mathcal{H}x_2$, $\frac{\partial(\mathcal{H}x_1)}{\partial \xi}$ and $\frac{\partial(\mathcal{H}x_2)}{\partial \xi}$ in a single vector, which we denote

$$\Phi_\partial(\mathcal{H}x) \coloneqq \begin{bmatrix} (\mathcal{H}x)(1,t) \\ \frac{\partial(\mathcal{H}x)}{\partial \xi}(1,t) \\ (\mathcal{H}x)(0,t) \\ \frac{\partial(\mathcal{H}x)}{\partial \xi}(0,t) \end{bmatrix} = \begin{bmatrix} \frac{1}{\rho a} x_1(1,t) \\ EI x_2(1,t) \\ \frac{1}{\rho a} \frac{\partial x_1}{\partial \xi}(1,t) \\ EI \frac{\partial x_2}{\partial \xi}(1,t) \\ \frac{1}{\rho a} x_1(0,t) \\ EI x_2(0,t) \\ \frac{1}{\rho a} \frac{\partial x_1}{\partial \xi}(0,t) \\ EI \frac{\partial x_2}{\partial \xi}(0,t) \end{bmatrix}. \tag{3.47}$$

Generally, we can express boundary conditions to (3.37) as linear combinations of the boundary values. In other words, we can express them as

$$W' \Phi_\partial(\mathcal{H}x) = 0, \qquad W' \in \mathbb{R}^{4 \times 8}. \tag{3.48}$$

Not all linear combinations are valid boundary conditions, however. In the following, we study the requirements for valid boundary conditions that generate contraction semigroups.

We can now construct the *boundary port variables* f_∂ (boundary flow) and e_∂ (boundary effort) as [2, p. 4]

$$\begin{bmatrix} f_{\partial,\mathcal{H}x} \\ e_{\partial,\mathcal{H}x} \end{bmatrix} \coloneqq \frac{1}{\sqrt{2}} \begin{bmatrix} Q & -Q \\ I & I \end{bmatrix} \Phi_\partial(\mathcal{H}x), \tag{3.49}$$

where

$$Q_{ij} = \begin{cases} (-1)^{j-1} P_{i+j-1}, & i + j \leq N + 1 \\ 0, & \text{else.} \end{cases} \tag{3.50}$$

We note that Q does not depend on P_0. For our system we have $N = 2$, so we have non-zero entries for $i + j \leq 3$ and we obtain $Q_{11} = P_1$, $Q_{12} = -P_2$, $Q_{21} = P_2$ and $Q_{22} = 0$.

Thus we get

$$Q = \begin{bmatrix} P_1 & -P_2 \\ P_2 & 0 \end{bmatrix} = \begin{bmatrix} & & & 1 \\ & & -1 & \\ & -1 & & \\ 1 & & & \end{bmatrix}. \tag{3.51}$$

We can now write

$$\frac{1}{\sqrt{2}} \begin{bmatrix} Q & -Q \\ I & I \end{bmatrix} = \frac{1}{\sqrt{2}} \begin{bmatrix} & & 1 & & & & -1 \\ & & & -1 & & 1 & \\ & -1 & & & 1 & & \\ 1 & & & & -1 & & \\ 1 & & & & 1 & & \\ & 1 & & & & 1 & \\ & & 1 & & & & 1 \\ & & & 1 & & & \end{bmatrix} =: R_{\text{ext}}. \tag{3.52}$$

We immediately see that R_{ext} is invertible. Finally, the boundary port variables become

$$\begin{bmatrix} f_{\partial,\mathcal{H}x} \\ e_{\partial,\mathcal{H}x} \end{bmatrix} = R_{\text{ext}} \Phi_\partial(\mathcal{H}x) = \frac{1}{\sqrt{2}} \begin{bmatrix} EI\frac{\partial x_2}{\partial \xi}(1,t) - EI\frac{\partial x_2}{\partial \xi}(0,t) \\ -\frac{1}{\rho a}\frac{\partial x_1}{\partial \xi}(1,t) + \frac{1}{\rho a}\frac{\partial x_1}{\partial \xi}(0,t) \\ -EIx_2(1,t) + EIx_2(0,t) \\ \frac{1}{\rho a}x_1(1,t) - \frac{1}{\rho a}x_1(0,t) \\ \frac{1}{\rho a}x_1(1,t) + \frac{1}{\rho a}x_1(0,t) \\ EIx_2(1,t) + EIx_2(0,t) \\ \frac{1}{\rho a}\frac{\partial x_1}{\partial \xi}(1,t) + \frac{1}{\rho a}\frac{\partial x_1}{\partial \xi}(0,t) \\ EI\frac{\partial x_2}{\partial \xi}(1,t) + EI\frac{\partial x_2}{\partial \xi}(0,t) \end{bmatrix}. \tag{3.53}$$

In order to consider generation of semigroups, we need to impose boundary conditions for (3.38). This is equivalent to imposing boundary conditions for

$$\frac{d}{dt}x(t) = P_2\frac{\partial^2}{\partial \xi^2}\big(\mathcal{H}x(t)\big) + P_1\frac{\partial}{\partial \xi}\big(\mathcal{H}x(t)\big) + P_0\big(\mathcal{H}x(t)\big) =: A_0 x(t). \tag{3.54}$$

We can describe suitable boundary conditions with a full-rank matrix $W \in \mathbb{R}^{4\times 8}$ such that

$$W \begin{bmatrix} f_{\partial,\mathcal{H}x} \\ e_{\partial,\mathcal{H}x} \end{bmatrix} = 0. \tag{3.55}$$

Using W, we define the restricted operator A as

$$A = A_0|_{\mathcal{D}(A)} \qquad \text{with} \qquad \mathcal{D}(A) = \left\{ x \in \mathcal{D}(A_0) \;\middle|\; W \begin{bmatrix} f_{\partial,\mathcal{H}x} \\ e_{\partial,\mathcal{H}x} \end{bmatrix} = 0 \right\}. \tag{3.56}$$

The following theorem states sufficient conditions for when A generates a contraction semigroup.

Theorem 3.2. Assume W is a full-rank matrix describing boundary conditions in terms of the boundary port variables in (3.55) and A is as in (3.56). If

$$W\Sigma W^* \geq 0 \qquad \text{and} \qquad \operatorname{Re} P_0 \leq 0, \tag{3.57}$$

where $\Sigma = \left[\begin{smallmatrix} 0 & I \\ I & 0 \end{smallmatrix}\right]$, then A generates a contraction semigroup and has a compact resolvent.

Proof. A proof is given in [2, Theorem 2.3], which is partly based on [8]. □

Since $P_0 = \left[\begin{smallmatrix} -\gamma & 0 \\ 0 & 0 \end{smallmatrix}\right]$ with $\gamma > 0$, for our system, the latter condition is satisfied. Furthermore, we can express the boundary conditions in terms of $\Phi_\partial(\mathcal{H}x)$:

$$0 = W \begin{bmatrix} f_{\partial,\mathcal{H}x} \\ e_{\partial,\mathcal{H}x} \end{bmatrix} = W R_{\text{ext}} \Phi_\partial(\mathcal{H}x) = W' \Phi_\partial(\mathcal{H}x), \tag{3.58}$$

where $W' = W R_{\text{ext}}$. Because R_{ext} is invertible, we can solve for W if we know W'. Thus it does not matter whether we express the boundary conditions in terms of the boundary port variables or the boundary value vector $\Phi_\partial(\mathcal{H}x)$.

4 SPECTRAL GALERKIN METHOD FOR ONE EULER–BERNOULLI BEAM

In this chapter, we develop a spectral Galerkin method for simulating a single Euler–Bernoulli beam. In particular, we cover two cases of boundary controlled beams—a simply supported beam with a single boundary control input at $\xi = 0$ and a cantilevered beam with two boundary control inputs at $\xi = 0$. The latter case corresponds to the beam model we will eventually use for approximating a flexible satellite in chapter 5.

The first section is a brief introduction to weighted residual methods and modal basis functions, which form the core of spectral methods in general. The following three sections cover the derivation of the spectral Galerkin approximation for the two boundary controlled beams. For the reader's convenience, the use of Legendre polynomials as modal basis functions is covered in a separate section. At the end of this chapter, we represent worked simulations for the two cases of boundary controlled beams.

4.1 Weighted Residual Methods and Modal Basis Functions

This section serves as a brief introduction to *weighted residual methods*, which are a class of approximate methods for discretising the spatial domain in linear ordinary and partial differential equations. In particular, using a weighted residual method, a linear partial differential equation can be approximated with a system of linear ordinary differential equations depending only on time. We demonstrate the idea of weighted residual methods with the following example. Weighted residual methods are covered more generally in [17, pp. 1–3].

Example 4.1. Consider a static beam of homogeneous material on $[0, 1]$ that is horizontally clamped at both ends, with load distribution $q \in L^2([0, 1]; \mathbb{R})$. The governing equations are

$$EI\frac{d^4w}{d\xi^4}(\xi) = q(\xi), \qquad w(0) = w(1) = \frac{dw}{d\xi}(0) = \frac{dw}{d\xi}(1) = 0. \tag{4.1}$$

We approximate the solution with $w^N(\xi) = \sum_{k=0}^{N} \alpha_k \phi_k(\xi)$, where $\alpha_k \in \mathbb{R}$ and $\phi_k \in V_N$, where V_N is a suitable subspace of a vector space X. The functions ϕ_k are called *modal basis functions*. Let $\psi_m \in V_N' \subset X$ be our *test functions*. We take V_N and V_N' to be finite subspaces, in this case $N + 1$ -dimensional. We may express the governing ordinary

differential equation as

$$\left\langle EI\frac{d^4w}{d\xi^4} - q, \psi \right\rangle_X = 0, \tag{4.2}$$

where $\langle \cdot, \cdot \rangle_X$ is an inner product defined on X. We assume this inner product is linear in both arguments for real functions. In this equation, we substitute w^N in place of w and $\psi_m \in V_N'$ in place of ψ to obtain

$$EI\sum_{k=0}^{N} \alpha_k \left\langle \frac{d^4\phi_k}{d\xi^4}, \psi_m \right\rangle_X = \langle q, \psi_m \rangle_X, \qquad m = 0, 1, \ldots, N. \tag{4.3}$$

This is a linear system which we can solve for the coefficients α_k to obtain an approximate solution w^N. We require the modal basis functions to be such that they satisfy the original ordinary differential equation and its boundary conditions. In other words, we require ϕ_k to satisfy

$$\phi_k \in \left\{ f \in C^4([0,1];\mathbb{R}) \;\middle|\; f(0) = f(1) = \frac{df}{d\xi}(0) = \frac{df}{d\xi}(1) = 0 \right\} \tag{4.4}$$

for all $k = 0, 1, \ldots, N$.

For linear partial differential equations in ξ and t, we assume the approximate solution to be of the form $w^N(\xi, t) = \sum_{k=0}^{N} \alpha_k(t)\phi_k(\xi)$. Then following a similar procedure using test functions and a suitable inner product, we obtain a system of linear ordinary differential equations in time. In this work, we are exclusively interested in the *Galerkin method*, which takes the modal basis and test functions to be the same, i.e. $\phi_j = \psi_j$ for all $j = 0, 1, \ldots, N$. In particular, we will be using the Legendre polynomials as building blocks for our basis functions, which means we can use the standard L^2-inner product.

We see from (4.4) that any linear combination of the modal basis functions satisfies the boundary conditions. This is a central property of modal basis functions in general. In order to obtain a unique modal basis function representation, the modal basis functions must be linearly independent. The general idea is that when more modal basis functions are used for the approximation, the approximate solution to a differential equation becomes increasingly accurate. Naturally, this only works if a set of (infinitely many) modal basis functions can be used to approximate the exact solution to an arbitrary precision. For Legendre polynomials, this is true, as any function that is continuous on the whole interval $[0, 1]$ has a pointwise convergent Legendre series expansion, based on [11, Theorem 7.11]. Because the Legendre polynomials are mutually orthogonal, they are also linearly independent. A set of modal basis functions satisfying the requirements in example 4.1 is given by

$$\phi_k(\xi) = L_k(\xi) - \frac{4k+10}{2k+7}L_{k+2}(\xi) + \frac{2k+3}{2k+7}L_{k+4}(\xi), \qquad k \in \mathbb{N}, \quad \xi \in [0,1], \tag{4.5}$$

where L_j is the j-th shifted Legendre polynomial. The first six of these basis functions are shown in figure 4.1.

Similarly, the modal basis function approach can be applied to problems with non-homo-

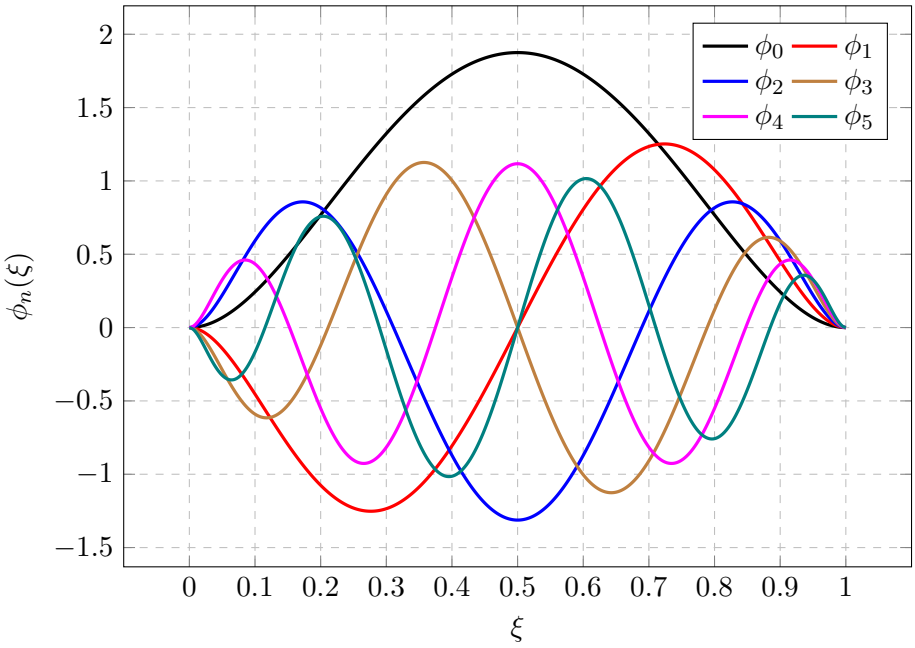

Figure 4.1. *The first six basis functions of the form* $L_k - \frac{4k+10}{2k+7}L_{k+2} + \frac{2k+3}{2k+7}L_{k+4}$.

geneous boundary conditions. For example, suppose our problem is the same as in (4.1) but we have $\frac{dw}{d\xi}(0) = b \neq 0$ instead of the homogeneous boundary condition. We use the same set of modal basis functions as we did for homogeneous boundary conditions, but add in a single, different basis function that satisfies the homogeneous boundary conditions $w(0) = w(1) = \frac{dw}{d\xi}(1) = 0$ and a non-zero boundary condition $\frac{dw}{d\xi}(0) = 1$. We denote the "homogeneous" part of the modal basis function set by $\{\phi_k\}_{k=0}^{N-1}$ and the different basis function by ϕ_N. A simple polynomial satisfying these boundary conditions is $\phi_N(\xi) = \xi^3 - 2\xi^2 + \xi$.

With this approach, the non-zero boundary value is represented in the approximation $w^N(\xi) = \sum_{k=0}^{N} \alpha_k \phi_k(\xi)$ solely by the single basis function ϕ_N and its coefficient α_N. This has the advantage of allowing us to construct a modal basis function set first assuming homogeneous boundary conditions and then adding a specific basis function for approximating each non-zero boundary value. This idea extends to approximating partial differential equations with $w^N(\xi, t) = \sum_{k=0}^{N} \alpha_k(t)\phi_k(\xi)$ instead.

4.2 Semidiscretisation of the Energy Space Formulation

In order to obtain a numerical method for approximating (3.35), we perform semidiscretisation to the system to eliminate the spatial variable ξ and obtain a system of linear first-order ordinary differential equations in time. Let $\psi \in V_1$ and $\Psi \in V_2$ be our test functions, where V_1, V_2 are suitable vector spaces to be defined later. Taking L^2-inner products of both sides of the equations, first equation with ψ and the second with Ψ, we

get

$$\begin{cases} \left\langle \dfrac{\partial x_1}{\partial t}(\cdot,t),\psi \right\rangle_{L^2} = -\dfrac{\gamma}{\rho a}\langle x_1(\cdot,t),\psi\rangle_{L^2} - EI\left\langle \dfrac{\partial^2 x_2}{\partial \xi^2}(\cdot,t),\psi \right\rangle_{L^2} \\ \left\langle \dfrac{\partial x_2}{\partial t}(\cdot,t),\Psi \right\rangle_{L^2} = \dfrac{1}{\rho a}\left\langle \dfrac{\partial^2 x_1}{\partial \xi^2}(\cdot,t),\Psi \right\rangle_{L^2}, \end{cases} \tag{4.6}$$

where we have used the fact that the inner product in $L^2([0,1];\mathbb{R})$ is linear in both arguments. We apply the weighted residual method. Let $\{\phi_k\}_{k=0}^N$ and $\{\Phi_k\}_{k=0}^N$ be our sets of modal basis functions for approximating x_1 and x_2 in the following way:

$$x_1(\xi,t) \approx \sum_{k=0}^{N} \alpha_k(t)\phi_k(\xi) \qquad \text{and} \qquad x_2(\xi,t) \approx \sum_{k=0}^{N} \beta_k(t)\Phi_k(\xi), \tag{4.7}$$

where $\alpha_k \colon (0,\infty) \to \mathbb{R}$ and $\beta_k \colon (0,\infty) \to \mathbb{R}$ are the coefficient functions to be determined. The reason we start the indexing at $k = 0$ lies in the definition of the Legendre polynomials, as the indexing for them also starts at zero. This makes our notations involving the modal basis function approximations more natural.

We proceed by applying the Galerkin method [17, pp. 6–7] to (4.6). This means we take the test and modal basis functions to be the same, namely $V_1 = \{\psi_k\}_{k=0}^N = \{\phi_k\}_{k=0}^N$ and $V_2 = \{\Psi_k\}_{k=0}^N = \{\Phi_k\}_{k=0}^N$. We get $N+1$ equations of the form of (4.6), for each ψ_m, Ψ_m with $m \in 0, 1, \ldots, N$. Let us consider the left hand sides of the equations first. We get

$$\left\langle \frac{\partial x_1}{\partial t}(\cdot,t),\psi_m \right\rangle_{L^2} \approx \left\langle \frac{\partial}{\partial t}\sum_{k=0}^{N} \alpha_k(t)\phi_k(\cdot),\psi_m \right\rangle_{L^2} = \sum_{k=0}^{N} \langle \phi_k,\psi_m\rangle_{L^2} \frac{d}{dt}\alpha_k(t), \tag{4.8}$$

where $\langle \phi_k,\psi_m\rangle_{L^2} = \int_0^1 \phi_k(\xi)\psi_m(\xi)\,d\xi$. Similarly, we have

$$\left\langle \frac{\partial x_2}{\partial t}(\cdot,t),\Psi_m \right\rangle_{L^2} \approx \sum_{k=0}^{N} \langle \Phi_k,\Psi_m\rangle_{L^2} \frac{d}{dt}\beta_k(t). \tag{4.9}$$

We can write these equations in matrix form in the following way. Assume (4.8) denotes row index m of a matrix resulting from matrix–vector multiplication. We may write

$$\sum_{k=0}^{N} \langle \phi_k,\psi_m\rangle_{L^2} \frac{d}{dt}\alpha_k(t) = \begin{bmatrix} \langle \phi_0,\psi_m\rangle_{L^2} & \langle \phi_1,\psi_m\rangle_{L^2} & \cdots & \langle \phi_N,\psi_m\rangle_{L^2} \end{bmatrix} \begin{bmatrix} \frac{d}{dt}\alpha_0(t) \\ \frac{d}{dt}\alpha_1(t) \\ \vdots \\ \frac{d}{dt}\alpha_N(t) \end{bmatrix}. \tag{4.10}$$

The full matrix formulation consists of all the rows. Knowing that $\phi_j = \psi_j$ for all j, we have

$$\begin{bmatrix} \langle \phi_0, \phi_0 \rangle_{L^2} & \langle \phi_1, \phi_0 \rangle_{L^2} & \cdots & \langle \phi_N, \phi_0 \rangle_{L^2} \\ \langle \phi_0, \phi_1 \rangle_{L^2} & \langle \phi_1, \phi_1 \rangle_{L^2} & \cdots & \langle \phi_N, \phi_1 \rangle_{L^2} \\ \vdots & \vdots & \ddots & \vdots \\ \langle \phi_0, \phi_N \rangle_{L^2} & \langle \phi_1, \phi_N \rangle_{L^2} & \cdots & \langle \phi_N, \phi_N \rangle_{L^2} \end{bmatrix} \begin{bmatrix} \frac{d}{dt}\alpha_0(t) \\ \frac{d}{dt}\alpha_1(t) \\ \vdots \\ \frac{d}{dt}\alpha_N(t) \end{bmatrix} =: M_1 \frac{d}{dt}\alpha(t), \tag{4.11}$$

where M_1 is often called the *mass matrix*. Note that as the inner product in $L^2([0,1];\mathbb{R})$ is symmetric, the matrix M_1 is symmetric. This is a useful property of the Galerkin method. In the same vein having $\Phi_j = \Psi_j$ for all j, we can transform (4.9) into a matrix–vector product and obtain a similar matrix formulation, namely

$$\begin{bmatrix} \langle \Phi_0, \Phi_0 \rangle_{L^2} & \langle \Phi_1, \Phi_0 \rangle_{L^2} & \cdots & \langle \Phi_N, \Phi_0 \rangle_{L^2} \\ \langle \Phi_0, \Phi_1 \rangle_{L^2} & \langle \Phi_1, \Phi_1 \rangle_{L^2} & \cdots & \langle \Phi_N, \Phi_1 \rangle_{L^2} \\ \vdots & \vdots & \ddots & \vdots \\ \langle \Phi_0, \Phi_N \rangle_{L^2} & \langle \Phi_1, \Phi_N \rangle_{L^2} & \cdots & \langle \Phi_N, \Phi_N \rangle_{L^2} \end{bmatrix} \begin{bmatrix} \frac{d}{dt}\beta_0(t) \\ \frac{d}{dt}\beta_1(t) \\ \vdots \\ \frac{d}{dt}\beta_N(t) \end{bmatrix} =: M_2 \frac{d}{dt}\beta(t). \tag{4.12}$$

With the same reasoning as before, we notice that M_2 is also a symmetric matrix. Furthermore, we can combine the two into a single block matrix form

$$\begin{bmatrix} M_1 & 0 \\ 0 & M_2 \end{bmatrix} \begin{bmatrix} \frac{d}{dt}\alpha(t) \\ \frac{d}{dt}\beta(t) \end{bmatrix} =: M \frac{d}{dt}\tilde{x}(t). \tag{4.13}$$

Because M_1 and M_2 are symmetric, the combined block matrix M is also symmetric. Additionally, M is invertible if and only if M_1 and M_2 are invertible.

Handling the right hand sides of (4.6) is not quite as straightforward and depends on our boundary conditions and choice of boundary input variables. We will do the necessary computations in steps. Let us denote

$$r_1^m(t) \coloneqq \left\langle x_1(\cdot,t), \psi_m \right\rangle_{L^2} \tag{4.14}$$

$$r_2^m(t) \coloneqq \left\langle \frac{\partial^2 x_2}{\partial \xi^2}(\cdot,t), \psi_m \right\rangle_{L^2} \tag{4.15}$$

$$r_3^m(t) \coloneqq \left\langle \frac{\partial^2 x_1}{\partial \xi^2}(\cdot,t), \Psi_m \right\rangle_{L^2}. \tag{4.16}$$

In order to include boundary control input, we need to have the necessary boundary terms first. We get the boundary terms of x_1 and x_2 by integrating r_2^m and r_3^m by parts.

First we integrate r_2^m by parts twice to obtain

$$\begin{aligned}
r_2^m(t) &= \int_0^1 \frac{\partial^2 x_2}{\partial \xi^2}(\xi,t)\psi_m(\xi)\,d\xi \\
&= \left[\frac{\partial x_2}{\partial \xi}(\xi,t)\psi_m(\xi)\right]_0^1 - \int_0^1 \frac{\partial x_2}{\partial \xi}(\xi,t)\frac{d\psi_m}{d\xi}(\xi)\,d\xi \\
&= \left[\frac{\partial x_2}{\partial \xi}(\xi,t)\psi_m(\xi)\right]_0^1 - \left(\left[x_2(\xi,t)\frac{d\psi_m}{d\xi}(\xi)\right]_0^1 - \int_0^1 x_2(\xi,t)\frac{d^2\psi_m}{d\xi^2}(\xi)\,d\xi\right) \\
&= \int_0^1 x_2(\xi,t)\frac{d^2\psi_m}{d\xi^2}(\xi)\,d\xi + \left[\frac{\partial x_2}{\partial \xi}(\xi,t)\psi_m(\xi)\right]_0^1 - \left[x_2(\xi,t)\frac{d\psi_m}{d\xi}(\xi)\right]_0^1 \\
&= \left\langle x_2(\cdot,t), \frac{d^2\psi_m}{d\xi^2}\right\rangle_{L^2} + \frac{\partial x_2}{\partial \xi}(1,t)\psi_m(1) - \frac{\partial x_2}{\partial \xi}(0,t)\psi_m(0) \\
&\qquad - x_2(1,t)\frac{d\psi_m}{d\xi}(1) + x_2(0,t)\frac{d\psi_m}{d\xi}(0) \\
&\approx \sum_{k=0}^{N}\left\langle \Phi_k, \frac{d^2\psi_m}{d\xi^2}\right\rangle_{L^2}\beta_k(t) + \frac{\partial x_2}{\partial \xi}(1,t)\psi_m(1) - \frac{\partial x_2}{\partial \xi}(0,t)\psi_m(0) \\
&\qquad - x_2(1,t)\frac{d\psi_m}{d\xi}(1) + x_2(0,t)\frac{d\psi_m}{d\xi}(0).
\end{aligned}$$

Because the formulation of r_3^m is similar to that of r_2^m, we get

$$\begin{aligned}
r_3^m(t) \approx \sum_{k=0}^{N}\left\langle \phi_k, \frac{d^2\Psi_m}{d\xi^2}\right\rangle_{L^2}\alpha_k(t) + \frac{\partial x_1}{\partial \xi}(1,t)\Psi_m(1) - \frac{\partial x_1}{\partial \xi}(0,t)\Psi_m(0) \\
- x_1(1,t)\frac{d\Psi_m}{d\xi}(1) + x_1(0,t)\frac{d\Psi_m}{d\xi}(0).
\end{aligned}$$

Lastly, for r_1^m we get simply

$$r_1^m(t) \approx \sum_{k=0}^{N}\langle \phi_k, \psi_m\rangle_{L^2}\alpha_k(t). \tag{4.17}$$

Because $\phi_j = \psi_j$ for all $j \in \{0,1,\ldots,N\}$, we can express this in vector form as

$$r_1^m(t) \approx \begin{bmatrix}\langle \phi_0,\phi_m\rangle_{L^2} & \langle \phi_1,\phi_m\rangle_{L^2} & \cdots & \langle \phi_N,\phi_m\rangle_{L^2}\end{bmatrix}\begin{bmatrix}\alpha_0(t)\\ \alpha_1(t)\\ \vdots \\ \alpha_N(t)\end{bmatrix}. \tag{4.18}$$

Combining all of these into a single matrix–vector product for all $m \in \{0,1,\ldots,N\}$, we

obtain the expression $-\frac{\gamma}{\rho a} r_1^m(t) \approx K_1 \alpha(t)$, where

$$K_1 = -\frac{\gamma}{\rho a} \begin{bmatrix} \langle \phi_0, \phi_0 \rangle_{L^2} & \langle \phi_1, \phi_0 \rangle_{L^2} & \cdots & \langle \phi_N, \phi_0 \rangle_{L^2} \\ \langle \phi_0, \phi_1 \rangle_{L^2} & \langle \phi_1, \phi_1 \rangle_{L^2} & \cdots & \langle \phi_N, \phi_1 \rangle_{L^2} \\ \vdots & \vdots & \ddots & \vdots \\ \langle \phi_0, \phi_N \rangle_{L^2} & \langle \phi_1, \phi_N \rangle_{L^2} & \cdots & \langle \phi_N, \phi_N \rangle_{L^2} \end{bmatrix} \quad \text{and} \quad \alpha(t) = \begin{bmatrix} \alpha_0(t) \\ \alpha_1(t) \\ \vdots \\ \alpha_N(t) \end{bmatrix}. \tag{4.19}$$

We split further processing of r_2^m and r_3^m into two separate sections. The first one covers a boundary controlled system based on a simply supported beam, and the second one covers a boundary controlled system based on a cantilevered beam. We do this because the matrix formulations obtained depend on the boundary conditions.

4.3 Simply Supported Beam with Boundary Control

The homogeneous boundary conditions for a simply supported dynamic beam are

$$w(0,t) = w(1,t) = \frac{\partial^2 w}{\partial \xi^2}(0,t) = \frac{\partial^2 w}{\partial \xi^2}(1,t) = 0. \tag{4.20}$$

We wish to control the bending moment at $\xi = 0$ with a function $u \in C([0,1];\mathbb{R})$. Because $x_2(0,t)$ represents the bending moment directly in terms of the energy variables, we get the boundary conditions

$$\begin{cases} x_1(0,t) = 0 \\ x_1(1,t) = 0 \\ x_2(0,t) = u(t) \\ x_2(1,t) = 0. \end{cases} \tag{4.21}$$

Because we have homogeneous boundary conditions for the variable x_1, the modal basis functions ϕ_k used for approximating it take the same boundary values $\phi_k(0) = \phi_k(1) = 0$ for all $k \in \{0, 1, \ldots, N\}$. Thus r_2^m simplifies to

$$r_2^m(t) \approx \sum_{k=0}^{N} \left\langle \Psi_k, \frac{d^2 \psi_m}{d\xi^2} \right\rangle_{L^2} \beta_k(t) + u(t) \frac{d\psi_m}{d\xi}(0). \tag{4.22}$$

For the variable x_2, we have $\Phi_k(0) = \Phi_k(1) = 0$ for $k \in \{0, 1, \ldots, N-1\}$. For applying boundary control, we use Φ_N such that $\Phi_N(0) \neq 0$ and $\Phi_N(1) = 0$. We have no need for the boundary terms of the variable x_1, so we may simply use (4.16) for r_3^m. Substituting in the approximation $x_1(\xi,t) \approx \sum_{k=0}^{N} \alpha_k(t)\phi_k(\xi)$, we obtain

$$r_3^m(t) \approx \sum_{k=0}^{N} \left\langle \frac{d^2 \phi_k}{d\xi^2}, \Psi_m \right\rangle_{L^2} \alpha_k(t). \tag{4.23}$$

Similarly to (4.19), we obtain the expression $-EIr_2^m(t) \approx K_2\beta(t) + B_2u(t)$, where

$$K_2 = -EI \begin{bmatrix} \left\langle \Phi_0, \frac{d^2\phi_0}{d\xi^2} \right\rangle_{L^2} & \left\langle \Phi_1, \frac{d^2\phi_0}{d\xi^2} \right\rangle_{L^2} & \cdots & \left\langle \Phi_N, \frac{d^2\phi_0}{d\xi^2} \right\rangle_{L^2} \\ \left\langle \Phi_0, \frac{d^2\phi_1}{d\xi^2} \right\rangle_{L^2} & \left\langle \Phi_1, \frac{d^2\phi_1}{d\xi^2} \right\rangle_{L^2} & \cdots & \left\langle \Phi_N, \frac{d^2\phi_1}{d\xi^2} \right\rangle_{L^2} \\ \vdots & \vdots & \ddots & \vdots \\ \left\langle \Phi_0, \frac{d^2\phi_N}{d\xi^2} \right\rangle_{L^2} & \left\langle \Phi_1, \frac{d^2\phi_N}{d\xi^2} \right\rangle_{L^2} & \cdots & \left\langle \Phi_N, \frac{d^2\phi_N}{d\xi^2} \right\rangle_{L^2} \end{bmatrix}, \tag{4.24}$$

$$\beta(t) = \begin{bmatrix} \beta_0(t) \\ \beta_1(t) \\ \vdots \\ \beta_N(t) \end{bmatrix} \quad \text{and} \quad B_1 = -EI \begin{bmatrix} \frac{d\phi_0}{d\xi}(0) \\ \frac{d\phi_1}{d\xi}(0) \\ \vdots \\ \frac{d\phi_N}{d\xi}(0) \end{bmatrix}. \tag{4.25}$$

In the same vein, we obtain the expression $\frac{1}{\rho a} r_3^m(t) \approx K_3\alpha(t)$, where

$$K_3 = \frac{1}{\rho a} \begin{bmatrix} \left\langle \frac{d^2\phi_0}{d\xi^2}, \Phi_0 \right\rangle_{L^2} & \left\langle \frac{d^2\phi_1}{d\xi^2}, \Phi_0 \right\rangle_{L^2} & \cdots & \left\langle \frac{d^2\phi_N}{d\xi^2}, \Phi_0 \right\rangle_{L^2} \\ \left\langle \frac{d^2\phi_0}{d\xi^2}, \Phi_1 \right\rangle_{L^2} & \left\langle \frac{d^2\phi_1}{d\xi^2}, \Phi_1 \right\rangle_{L^2} & \cdots & \left\langle \frac{d^2\phi_N}{d\xi^2}, \Phi_1 \right\rangle_{L^2} \\ \vdots & \vdots & \ddots & \vdots \\ \left\langle \frac{d^2\phi_0}{d\xi^2}, \Phi_N \right\rangle_{L^2} & \left\langle \frac{d^2\phi_1}{d\xi^2}, \Phi_N \right\rangle_{L^2} & \cdots & \left\langle \frac{d^2\phi_N}{d\xi^2}, \Phi_N \right\rangle_{L^2} \end{bmatrix} \tag{4.26}$$

and $\alpha(t)$ is the same as in (4.19). Finally, we can express (4.6) as a linear system for a boundary controlled simply supported beam as

$$\begin{cases} M\dfrac{d}{dt}\tilde{x}(t) = K\tilde{x}(t) + Bu(t) \\ \qquad \tilde{x}(0) = \tilde{x}_0 \in \mathbb{R}^{2N+2}, \end{cases} \tag{4.27}$$

where M and $\tilde{x}$ are as in (4.13) and

$$K = \begin{bmatrix} K_1 & K_2 \\ 0 & K_3 \end{bmatrix} \quad \text{and} \quad B = \begin{bmatrix} B_1 \\ 0 \end{bmatrix} \in \mathbb{R}^{2N+2}. \tag{4.28}$$

We obtain the initial condition $\tilde{x}_0$ as follows. Suppose w_0 and w_1 denote the initial deflection profile and velocity of the beam. Then using (3.36), we obtain the approximations

$$x_1(\xi, 0) = \rho a w_1(\xi) \approx \sum_{k=0}^{N} \alpha_k(0)\phi_k(\xi) \tag{4.29}$$

$$x_2(\xi, 0) = \frac{d^2 w_0}{d\xi^2}(\xi) \approx \sum_{k=0}^{N} \beta_k(0)\Phi_k(\xi). \tag{4.30}$$

The initial state of our system is described by the values of $\alpha_k(0)$ and $\beta_k(0)$. In other words, we obtain the initial state by finding modal basis function approximations for $\rho a w_1$

and $\frac{d^2 w_0}{d\xi^2}$. Thus the initial condition is equal to

$$\tilde{x}_0 = \begin{bmatrix} \alpha(0) & \beta(0) \end{bmatrix}^\mathsf{T} = \begin{bmatrix} \alpha_0(0) & \alpha_1(0) & \cdots & \alpha_N(0) & \beta_0(0) & \beta_1(0) & \cdots & \beta_N(0) \end{bmatrix}^\mathsf{T}. \quad (4.31)$$

4.4 Cantilevered Beam with Boundary Control

The homogeneous boundary conditions for a cantilevered beam that is horizontally clamped at $\xi = 0$ are

$$w(0,t) = \frac{\partial w}{\partial \xi}(0,t) = \frac{\partial^2 w}{\partial \xi^2}(1,t) = \frac{\partial^3 w}{\partial \xi^3}(1,t) = 0. \quad (4.32)$$

In this case, we wish to control the time derivatives of the deflection and slope with functions $u_1, u_2 \in C^1([0,1];\mathbb{R})$. We get the boundary conditions

$$\begin{cases} x_1(0,t) = u_1(t) \\ \dfrac{\partial x_1}{\partial \xi}(0,t) = u_2(t) \\ x_2(1,t) = 0 \\ \dfrac{\partial x_2}{\partial \xi}(1,t) = 0. \end{cases} \quad (4.33)$$

Because we have homogeneous boundary conditions for the variable x_2, the modal basis functions Φ_k used for approximating it take the same boundary values $\Phi_k(1) = \frac{d\Phi_k}{d\xi}(1) = 0$ for all $k \in \{0, 1, \ldots, N\}$. Thus r_3^m simplifies to

$$r_3^m(t) \approx \sum_{k=0}^{N} \left\langle \phi_k, \frac{d^2 \Psi_m}{d\xi^2} \right\rangle_{L^2} + u_1(t) \frac{d\Psi_m}{d\xi}(0) - u_2(t) \Psi_m(0). \quad (4.34)$$

For the variable x_1, we have $\phi_k(0) = \frac{d\phi_k}{d\xi}(0) = 0$ for $k \in \{0, 1, \ldots, N-2\}$. For applying boundary control, we use ϕ_{N-1} and ϕ_N such that $\phi_{N-1}(0) \neq 0$, $\frac{d\phi_{N-1}}{d\xi}(0) = 0$, $\phi_N(0) = 0$ and $\frac{d\phi_N}{d\xi}(0) \neq 0$. We have no need for the boundary terms of the variable x_2, so we may simply use (4.15) for r_2^m. Substituting in the approximation $x_2(\xi,t) \approx \sum_{k=0}^{N} \beta_k(t) \Phi_k(\xi)$, we obtain

$$r_2^m(t) \approx \sum_{k=0}^{N} \left\langle \frac{d^2 \Phi_k}{d\xi^2}, \psi_m \right\rangle_{L^2} \beta_k(t). \quad (4.35)$$

Similarly to (4.19), we obtain the expression $-EIr_2^m(t) \approx K_2\beta(t)$, where

$$K_2 = -EI \begin{bmatrix} \left\langle \Phi_0, \frac{d^2\phi_0}{d\xi^2} \right\rangle_{L^2} & \left\langle \Phi_1, \frac{d^2\phi_0}{d\xi^2} \right\rangle_{L^2} & \cdots & \left\langle \Phi_N, \frac{d^2\phi_0}{d\xi^2} \right\rangle_{L^2} \\ \left\langle \Phi_0, \frac{d^2\phi_1}{d\xi^2} \right\rangle_{L^2} & \left\langle \Phi_1, \frac{d^2\phi_1}{d\xi^2} \right\rangle_{L^2} & \cdots & \left\langle \Phi_N, \frac{d^2\phi_1}{d\xi^2} \right\rangle_{L^2} \\ \vdots & \vdots & \ddots & \vdots \\ \left\langle \Phi_0, \frac{d^2\phi_N}{d\xi^2} \right\rangle_{L^2} & \left\langle \Phi_1, \frac{d^2\phi_N}{d\xi^2} \right\rangle_{L^2} & \cdots & \left\langle \Phi_N, \frac{d^2\phi_N}{d\xi^2} \right\rangle_{L^2} \end{bmatrix}, \tag{4.36}$$

$$\beta(t) = \begin{bmatrix} \beta_0(t) \\ \beta_1(t) \\ \vdots \\ \beta_N(t) \end{bmatrix}. \tag{4.37}$$

In the same vein, we obtain the expression $\frac{1}{\rho a} r_3^m(t) \approx K_3\alpha(t) + B_2u(t)$, where

$$K_3 = \frac{1}{\rho a} \begin{bmatrix} \left\langle \frac{d^2\phi_0}{d\xi^2}, \Phi_0 \right\rangle_{L^2} & \left\langle \frac{d^2\phi_1}{d\xi^2}, \Phi_0 \right\rangle_{L^2} & \cdots & \left\langle \frac{d^2\phi_N}{d\xi^2}, \Phi_0 \right\rangle_{L^2} \\ \left\langle \frac{d^2\phi_0}{d\xi^2}, \Phi_1 \right\rangle_{L^2} & \left\langle \frac{d^2\phi_1}{d\xi^2}, \Phi_1 \right\rangle_{L^2} & \cdots & \left\langle \frac{d^2\phi_N}{d\xi^2}, \Phi_1 \right\rangle_{L^2} \\ \vdots & \vdots & \ddots & \vdots \\ \left\langle \frac{d^2\phi_0}{d\xi^2}, \Phi_N \right\rangle_{L^2} & \left\langle \frac{d^2\phi_1}{d\xi^2}, \Phi_N \right\rangle_{L^2} & \cdots & \left\langle \frac{d^2\phi_N}{d\xi^2}, \Phi_N \right\rangle_{L^2} \end{bmatrix}, \tag{4.38}$$

$$B_2 = \frac{1}{\rho a} \begin{bmatrix} \frac{d\Phi_0}{d\xi}(0) & -\Phi_0(0) \\ \frac{d\Phi_1}{d\xi}(0) & -\Phi_1(0) \\ \vdots & \vdots \\ \frac{d\Phi_N}{d\xi}(0) & -\Phi_N(0) \end{bmatrix} \quad \text{and} \quad u(t) = \begin{bmatrix} u_1(t) \\ u_2(t) \end{bmatrix}. \tag{4.39}$$

Additionally, $\alpha(t)$ is the same as in (4.19). Finally, we can express (4.6) as a linear system for a boundary controlled cantilevered beam as

$$\begin{cases} M\dfrac{d}{dt}\tilde{x}(t) = K\tilde{x}(t) + Bu(t) \\ \qquad \tilde{x}(0) = \tilde{x}_0 \in \mathbb{R}^{2N+2}, \end{cases} \tag{4.40}$$

where M and $\tilde{x}$ are as in (4.13) and

$$K = \begin{bmatrix} K_1 & K_2 \\ 0 & K_3 \end{bmatrix} \quad \text{and} \quad B = \begin{bmatrix} 0 \\ B_2 \end{bmatrix} \in \mathbb{R}^{(2N+2)\times 2}. \tag{4.41}$$

We obtain the initial condition $\tilde{x}_0$ from the initial deflection profile w_0 and the initial velocity w_1 the same way as in the previous section.

4.5 Modal Basis Functions Utilising Legendre Polynomials

The beam equation has four boundary conditions, so we study modal basis functions of the form

$$\begin{aligned}\phi_n(\xi) &= c_n\big(L_n(\xi) + g_1(n)L_{n+1}(\xi) + g_2(n)L_{n+2}(\xi) + g_3(n)L_{n+3}(\xi) + g_4(n)L_{n+4}(\xi)\big)\\ &= c_n\left(L_n(\xi) + \sum_{k=1}^{4} g_k(n)L_{n+k}(\xi)\right),\end{aligned} \tag{4.42}$$

where $c_n \neq 0$ is a scaling coefficient depending on n. This general formulation is supported by Jie Shen's articles considering spectral Galerkin approximations for Legendre [15] and Chebyshev polynomials [16]. First we study how to obtain a modal basis function approximation for a continuous function f by applying the Fourier–Legendre series expansion.

We obtain a polynomial approximation of degree N for function $f \in C^0([0,1];\mathbb{R})$ by truncating the Fourier–Legendre series (2.18), namely

$$f(\xi) \approx f_N(\xi) \coloneqq \sum_{n=0}^{N} a_n L_n(\xi), \qquad a_n = (2n+1)\langle f, L_n\rangle_{L^2}. \tag{4.43}$$

However, we are more interested in obtaining a polynomial approximation in terms of basis functions described in (4.42). We start by writing

$$\begin{aligned}\hat{f}_M(\xi) &\coloneqq \sum_{n=0}^{M} b_n\phi_n(\xi)\\ &= \sum_{n=0}^{M} b_n c_n L_n(\xi) + \sum_{n=0}^{M} b_n c_n g_1(n) L_{n+1}(\xi) + \sum_{n=0}^{M} b_n c_n g_2(n) L_{n+2}(\xi)\\ &\qquad + \sum_{n=0}^{M} b_n c_n g_3(n) L_{n+3}(\xi) + \sum_{n=0}^{M} b_n c_n g_4(n) L_{n+4}(\xi),\end{aligned}$$

where b_n are the unknown coefficients. Expanding the sum we get

$$\begin{aligned}\hat{f}_M(\xi) = {} & b_0c_0L_0(\xi) + b_1c_1L_1(\xi) + b_2c_2L_2(\xi) + \ldots + b_Mc_ML_M(\xi)\\ & + b_0c_0g_1(0)L_1(\xi) + b_1c_1g_1(1)L_2(\xi) + b_2c_2g_1(2)L_3(\xi) + \ldots + b_Mc_Mg_1(M)L_{M+1}(\xi)\\ & + b_0c_0g_2(0)L_2(\xi) + b_1c_1g_2(1)L_3(\xi) + b_2c_2g_2(2)L_4(\xi) + \ldots + b_Mc_Mg_2(M)L_{M+2}(\xi)\\ & + b_0c_0g_3(0)L_3(\xi) + b_1c_1g_3(1)L_4(\xi) + b_2c_2g_3(2)L_5(\xi) + \ldots + b_Mc_Mg_3(M)L_{M+3}(\xi)\\ & + b_0c_0g_4(0)L_4(\xi) + b_1c_1g_4(1)L_5(\xi) + b_2c_2g_4(2)L_6(\xi) + \ldots + b_Mc_Mg_4(M)L_{M+4}(\xi).\end{aligned}$$

Looking at the expanded sum above, we see that we can write $\hat{f}_M(\xi) = \sum_{n=0}^{M+4} a_n L_n(\xi)$,

where

$$a_n = \begin{cases} b_0c_0, & n = 0 \\ b_0c_0g_1(0) + b_1c_1, & n = 1 \\ b_0c_0g_2(0) + b_1c_1g_1(1) + b_2c_2, & n = 2 \\ b_0c_0g_3(0) + b_1c_1g_2(1) + b_2c_2g_1(2) + b_3c_3, & n = 3 \\ b_{n-4}c_{n-4}g_4(n-4) + b_{n-3}c_{n-3}g_3(n-3) + b_{n-2}c_{n-2}g_2(n-2) & \\ \qquad + b_{n-1}c_{n-1}g_1(n-1) + b_nc_n, & 4 \le n \le M \\ b_{M-3}c_{M-3}g_4(M-3) + b_{M-2}c_{M-2}g_3(M-2) & \\ \qquad + b_{M-1}c_{M-1}g_2(M-1) + b_Mc_Mg_1(M), & n = M+1 \\ b_{M-2}c_{M-2}g_4(M-2) + b_{M-1}c_{M-1}g_3(M-1) + b_Mc_Mg_2(M), & n = M+2 \\ b_{M-1}c_{M-1}g_4(M-1) + b_Mc_Mg_3(M), & n = M+3 \\ b_Mc_Mg_4(M), & n = M+4. \end{cases}$$

Assuming we know the coefficients a_n, we get a linear system from the first $M+1$ equations, which is enough to solve for each b_n. We get the system

$$Hb = a, \tag{4.44}$$

where $a = \begin{bmatrix} a_0 & a_1 & \cdots & a_M \end{bmatrix}^\mathsf{T}$, $b = \begin{bmatrix} b_0 & b_1 & \cdots & b_M \end{bmatrix}^\mathsf{T}$ and $H = (h_{ij}) \in \mathbb{R}^{(M+1)\times(M+1)}$ is a lower triangular matrix with

$$h_{ij} = \begin{cases} c_{j-1}, & i = j \\ c_{j-1}g_1(j-1), & i = j+1 \\ c_{j-1}g_2(j-1), & i = j+2 \\ c_{j-1}g_3(j-1), & i = j+3 \\ c_{j-1}g_4(j-1), & i = j+4 \\ 0, & \text{else.} \end{cases} \tag{4.45}$$

Because H is a triangular matrix with non-zero diagonal entries ($c_n \neq 0$), it is invertible and thus (4.44) is solvable with $b = H^{-1}a$.

Let us denote

$$\begin{cases} x_1^N(\xi, t) \coloneqq \sum_{n=0}^{N} \alpha_n(t)\phi_n(\xi) \\ x_2^N(\xi, t) \coloneqq \sum_{n=0}^{N} \beta_n(t)\Phi_n(\xi) \end{cases} \tag{4.46}$$

and

$$x^N(\xi, t) \coloneqq \begin{bmatrix} x_1^N(\xi, t) \\ x_2^N(\xi, t) \end{bmatrix}. \tag{4.47}$$

Assume our boundary conditions for the homogeneous part of our modal basis function set are expressed in the form $W'\Phi_\partial(\mathcal{H}x) = 0$, where $W' \in \mathbb{R}^{4\times 8}$ satisfies the conditions

described in section 3.7. We address the boundary control part later. Substituting the approximation x^N in place of x, we obtain

$$W'\Phi_\partial\big(\mathcal{H}x^N\big) = 0. \tag{4.48}$$

Computing $\mathcal{H}x^N$, we get

$$\big(\mathcal{H}x^N\big)(\xi,t) = \begin{bmatrix} \frac{1}{\rho a} & 0 \\ 0 & EI \end{bmatrix} \begin{bmatrix} x_1^N(\xi,t) \\ x_2^N(\xi,t) \end{bmatrix} = \begin{bmatrix} \frac{1}{\rho a} x_1^N(\xi,t) \\ EI x_2^N(\xi,t) \end{bmatrix} = \begin{bmatrix} \frac{1}{\rho a}\sum_{n=0}^N \alpha_n(t)\phi_n(\xi) \\ EI\sum_{n=0}^N \beta_n(t)\Phi_n(\xi) \end{bmatrix}. \tag{4.49}$$

Similarly, we get

$$\frac{\partial}{\partial\xi}\big(\mathcal{H}x^N\big)(\xi,t) = \begin{bmatrix} \frac{1}{\rho a}\sum_{n=0}^N \alpha_n(t)\frac{d\phi_n}{d\xi}(\xi) \\ EI\sum_{n=0}^N \beta_n(t)\frac{d\Phi_n}{d\xi}(\xi) \end{bmatrix}. \tag{4.50}$$

Expanding (4.48), we obtain

$$W'\begin{bmatrix} \frac{1}{\rho a}\sum_{n=0}^N \alpha_n(t)\phi_n(1) \\ EI\sum_{n=0}^N \beta_n(t)\Phi_n(1) \\ \frac{1}{\rho a}\sum_{n=0}^N \alpha_n(t)\frac{d\phi_n}{d\xi}(1) \\ EI\sum_{n=0}^N \beta_n(t)\frac{d\Phi_n}{d\xi}(1) \\ \frac{1}{\rho a}\sum_{n=0}^N \alpha_n(t)\phi_n(0) \\ EI\sum_{n=0}^N \beta_n(t)\Phi_n(0) \\ \frac{1}{\rho a}\sum_{n=0}^N \alpha_n(t)\frac{d\phi_n}{d\xi}(0) \\ EI\sum_{n=0}^N \beta_n(t)\frac{d\Phi_n}{d\xi}(0) \end{bmatrix} = \sum_{n=0}^N W'\begin{bmatrix} \frac{1}{\rho a}\alpha_n(t)\phi_n(1) \\ EI\beta_n(t)\Phi_n(1) \\ \frac{1}{\rho a}\alpha_n(t)\frac{d\phi_n}{d\xi}(1) \\ EI\beta_n(t)\frac{d\Phi_n}{d\xi}(1) \\ \frac{1}{\rho a}\alpha_n(t)\phi_n(0) \\ EI\beta_n(t)\Phi_n(0) \\ \frac{1}{\rho a}\alpha_n(t)\frac{d\phi_n}{d\xi}(0) \\ EI\beta_n(t)\frac{d\Phi_n}{d\xi}(0) \end{bmatrix} = \begin{bmatrix} 0 \\ 0 \\ 0 \\ 0 \end{bmatrix}. \tag{4.51}$$

Because the boundary conditions need to apply at every time instant $t \in [0,\infty)$, the equation is independent of α_n and β_n. Furthermore, as the modal basis functions are linearly independent, the equation only holds if each term of the matrix sum equals zero.

This yields the condition

$$W' \begin{bmatrix} \mathcal{H} & & & \\ & \mathcal{H} & & \\ & & \mathcal{H} & \\ & & & \mathcal{H} \end{bmatrix} \begin{bmatrix} \phi_n(1) \\ \Phi_n(1) \\ \frac{d\phi_n}{d\xi}(1) \\ \frac{d\Phi_n}{d\xi}(1) \\ \phi_n(0) \\ \Phi_n(0) \\ \frac{d\phi_n}{d\xi}(0) \\ \frac{d\Phi_n}{d\xi}(0) \end{bmatrix} = \begin{bmatrix} 0 \\ 0 \\ 0 \\ 0 \end{bmatrix} \quad \text{for} \quad n = 0, 1, \ldots, N, \tag{4.52}$$

where we extracted $\mathcal{H} = \operatorname{diag}\left(\frac{1}{\rho a}, EI\right)$ out from each pair of terms for convenience. Denoting

$$\begin{cases} \phi_n(\xi) = c_n^1 \left(L_n(\xi) + \sum_{k=1}^{4} g_k^1(k) L_{n+k}(\xi) \right), \\ \Phi_n(\xi) = c_n^2 \left(L_n(\xi) + \sum_{k=1}^{4} g_k^2(k) L_{n+k}(\xi) \right), \end{cases} \tag{4.53}$$

we are able to expand the left hand side of (4.52). We get

$$W' \begin{bmatrix} \mathcal{H}C_n & & & \\ & \mathcal{H}C_n & & \\ & & \mathcal{H}C_n & \\ & & & \mathcal{H}C_n \end{bmatrix} \begin{bmatrix} L_n(1) + \sum_{k=1}^{4} g_k^1(n) L_{n+k}(1) \\ L_n(1) + \sum_{k=1}^{4} g_k^2(n) L_{n+k}(1) \\ \frac{dL_n}{d\xi}(1) + \sum_{k=1}^{4} g_k^1(n) \frac{dL_{n+k}}{d\xi}(1) \\ \frac{dL_n}{d\xi}(1) + \sum_{k=1}^{4} g_k^2(k) \frac{dL_{n+k}}{d\xi}(1) \\ L_n(0) + \sum_{k=1}^{4} g_k^1(n) L_{n+k}(0) \\ L_n(0) + \sum_{k=1}^{4} g_k^2(n) L_{n+k}(0) \\ \frac{dL_n}{d\xi}(0) + \sum_{k=1}^{4} g_k^1(n) \frac{dL_{n+k}}{d\xi}(0) \\ \frac{dL_n}{d\xi}(0) + \sum_{k=1}^{4} g_k^2(n) \frac{dL_{n+k}}{d\xi}(0) \end{bmatrix} = \begin{bmatrix} 0 \\ 0 \\ 0 \\ 0 \end{bmatrix}, \tag{4.54}$$

where $C_n = \operatorname{diag}\left(c_n^1, c_n^2\right)$, for all indices n. In order to obtain a matrix–vector equation, we

denote

$$\Lambda_n(\xi) \coloneqq \begin{bmatrix} L_n(\xi) & L_{n+1}(\xi) & L_{n+2}(\xi) & L_{n+3}(\xi) & L_{n+4}(\xi) \end{bmatrix}, \tag{4.55}$$

$$\Lambda'_n(\xi) \coloneqq \begin{bmatrix} \frac{dL_n}{d\xi}(\xi) & \frac{dL_{n+1}}{d\xi}(\xi) & \frac{dL_{n+2}}{d\xi}(\xi) & \frac{dL_{n+3}}{d\xi}(\xi) & \frac{dL_{n+4}}{d\xi}(\xi) \end{bmatrix}, \tag{4.56}$$

$$g(n) \coloneqq \begin{bmatrix} g^1(n) \\ g^2(n) \end{bmatrix}, \tag{4.57}$$

where $g^1(n) = \begin{bmatrix} 1 & g_1^1(n) & g_2^1(n) & g_3^1(n) & g_4^1(n) \end{bmatrix}^\mathsf{T}$ and $g^2(n) = \begin{bmatrix} 1 & g_1^2(n) & g_2^2(n) & g_3^2(n) & g_4^2(n) \end{bmatrix}^\mathsf{T}$. Finally, we get the equation

$$W' \begin{bmatrix} \mathcal{H}C_n & & & \\ & \mathcal{H}C_n & & \\ & & \mathcal{H}C_n & \\ & & & \mathcal{H}C_n \end{bmatrix} \begin{bmatrix} \Lambda_n(1) & 0 \\ 0 & \Lambda_n(1) \\ \Lambda'_n(1) & 0 \\ 0 & \Lambda'_n(1) \\ \Lambda_n(0) & 0 \\ 0 & \Lambda_n(0) \\ \Lambda'_n(0) & 0 \\ 0 & \Lambda'_n(0) \end{bmatrix} \begin{bmatrix} g^1(n) \\ g^2(n) \end{bmatrix} = \begin{bmatrix} 0 \\ 0 \\ 0 \\ 0 \end{bmatrix}, \tag{4.58}$$

which we aim to solve for $g^1(n)$ and $g^2(n)$ for each index n. The resulting system contains 8 unknown coefficients and 4 equations, making it an underdetermined system. Generally, we prefer solutions that yield polynomials of the least possible degree for the modal basis functions, for simpler numerical computations. Because we know the values of the Legendre polynomials and their derivatives at $\xi = 0$ and $\xi = 1$ (properties (ii) and (iii)), we get the following identities:

$$\Lambda_n(1) = \begin{bmatrix} 1 & 1 & 1 & 1 & 1 \end{bmatrix},$$

$$\Lambda'_n(1) = \begin{bmatrix} n^2+n & n^2+3n+2 & n^2+5n+6 & n^2+7n+12 & n^2+9n+20 \end{bmatrix},$$

$$\Lambda_n(0) = (-1)^n \begin{bmatrix} 1 & -1 & 1 & -1 & 1 \end{bmatrix},$$

$$\Lambda'_n(0) = (-1)^n \begin{bmatrix} -n^2-n & n^2+3n+2 & -n^2-5n-6 & n^2+7n+12 & -n^2-9n-20 \end{bmatrix}.$$

We yet have to address modal basis functions for applying boundary control input in our approximated system. We will do this for the boundary control inputs presented for the boundary controlled simply supported and cantilevered beams in the next section. Other kinds of boundary control inputs are not discussed in this work.

For modal basis functions for boundary control input, we choose to look for functions of

the form

$$\phi(\xi) = c_0 L_0(\xi) + c_1 L_1(\xi) + c_2 L_2(\xi), \tag{4.59}$$

which is a second-degree polynomial. For convenience, we want these basis functions to satisfy $\int_0^1 \phi(\xi)\, d\xi = 0$. For the boundary controlled simply supported beam, we control the value $x_2(0,t)$, other boundary conditions being homogeneous. Thus we look for a modal basis function of the form (4.59) satisfying $\Phi_N(0) = 1$ and $\Phi_N(1) = 0$. Applying the properties of Legendre polynomials and solving for the coefficients c_0, c_1 and c_2, we obtain

$$\Phi_N(\xi) = 0L_0(\xi) - \frac{1}{2}L_1(\xi) + \frac{1}{2}L_2(\xi) = 3\xi^2 - 4\xi + 1. \tag{4.60}$$

For the boundary controlled cantilevered beam, on the other hand, we control the values $x_1(0,t)$ and $\frac{\partial x_1}{\partial \xi}(0,t)$. We look for two modal basis functions of the form (4.59) that satisfy the conditions $\phi_{N-1}(0) = 1$, $\frac{d\phi_{N-1}}{d\xi}(0) = 0$, $\phi_N(0) = 0$ and $\frac{d\phi_N}{d\xi}(0) = 1$. Again solving for the coefficients c_0, c_1 and c_2 for both cases, we obtain

$$\begin{cases} \phi_{N-1}(\xi) = 0L_0(\xi) - \dfrac{3}{2}L_1(\xi) - \dfrac{1}{2}L_2(\xi) = -3\xi^2 + 1, \\ \phi_N(\xi) = 0L_0(\xi) - \dfrac{1}{4}L_1(\xi) - \dfrac{1}{4}L_2(\xi) = -\dfrac{3}{2}\xi^2 + \xi. \end{cases} \tag{4.61}$$

4.6 Simulation Example for a Single Beam

We simulate a cantilevered beam horizontally clamped at $\xi = 0$. Our physical parameters are $E = 1$, $I = 1$, $\rho = 10$, $a = 1$ and the viscous damping constant is $\gamma = 2$. We use 15 basis functions, thus we have $n = 0, 1, \ldots, 14$ for the basis functions ϕ_n and Φ_n. We simulate the beam for 20 seconds. Our initial deflection profile is

$$w_0(\xi) = \frac{1}{10}\big(\xi^4 - 4\xi^3 + 6\xi^2\big), \tag{4.62}$$

which satisfies the boundary conditions for a horizontally cantilevered beam. From this we obtain

$$\frac{d^2 w_0}{d\xi^2}(\xi) = \frac{1}{10}\big(12\xi^2 - 24\xi + 12\big), \tag{4.63}$$

which is our initial condition $x_2(\xi, 0)$, see (3.36). We assume our beam is at rest initially, so $x_1(\xi, 0) \equiv 0$. We solve for the corresponding basis function coefficients α_k and β_k for the spectral approximations $x_1(\xi,t) \approx \sum_{k=0}^N \alpha_k(t)\phi_k(\xi)$ and $x_2(\xi,t) \approx \sum_{k=0}^N \beta_k(t)\Phi_k(\xi)$ at $t = 0$.

We can solve for the deflection profile using numerical integration, as

$$x_1(\xi,t) = \rho a \frac{\partial w}{\partial t}(\xi,t) \quad \Leftrightarrow \quad \frac{\partial w}{\partial t}(\xi,t) = \frac{1}{\rho a} x_1(\xi,t) \approx \frac{1}{\rho a}\sum_{k=0}^{N} \phi_k(\xi)\alpha_k(t),$$

from which we obtain

$$w(\xi, T) \approx w(\xi, 0) + \frac{1}{\rho a} \sum_{k=0}^{N} \phi_k(\xi) \int_0^T \alpha_k(t)\, dt, \tag{4.64}$$

where $T \in [0, 20]$. Because the simulation only returns the values of $\alpha_k(t)$ at discrete time points, we approximate the integral by the trapezoidal rule for each computed time step T. We simulate the beam both with zero boundary input and boundary input of $\rho a \frac{\partial w}{\partial \xi \partial t}(0, t) = \frac{\partial x_1}{\partial t}(0, t) = -\sin(2\pi t)$. The beam without boundary control input is shown in figure 4.2, and with boundary control input in figure 4.3.

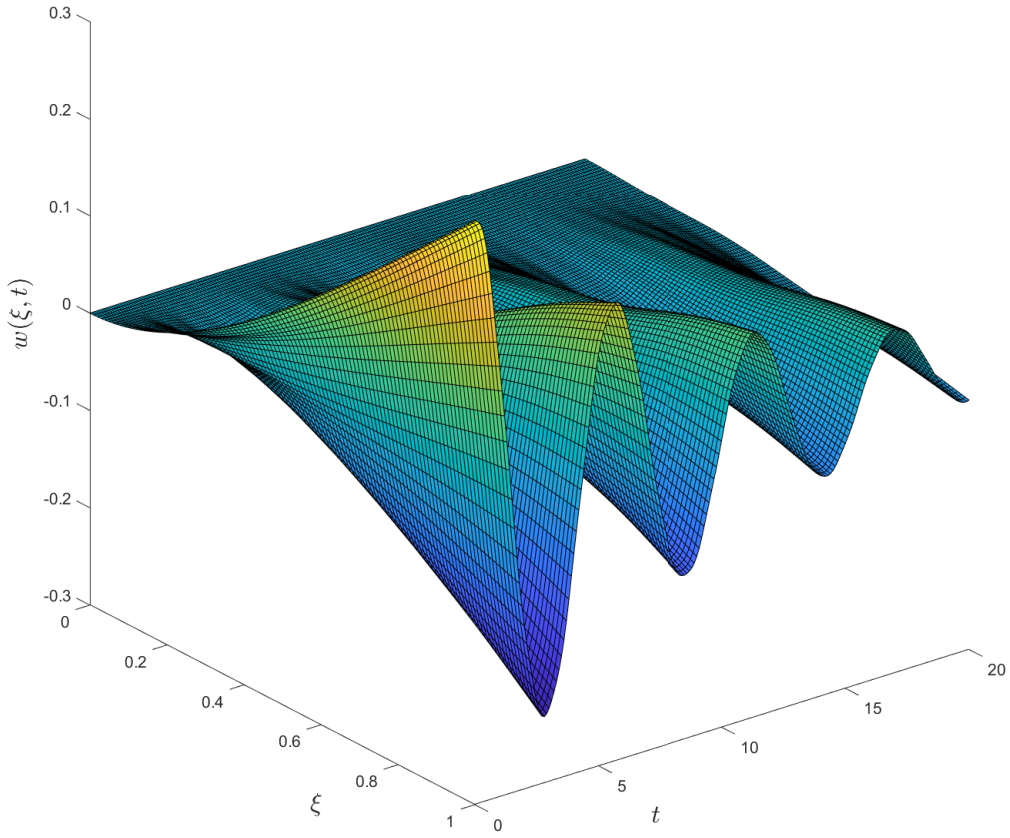

Figure 4.2. *A cantilevered beam without boundary control input.*

We see that without boundary control input, the vibration of the beam is dominated by the lowest frequency components. On the other hand, the periodic boundary control input adds higher frequency oscillation to the beam that is of relatively small amplitude.

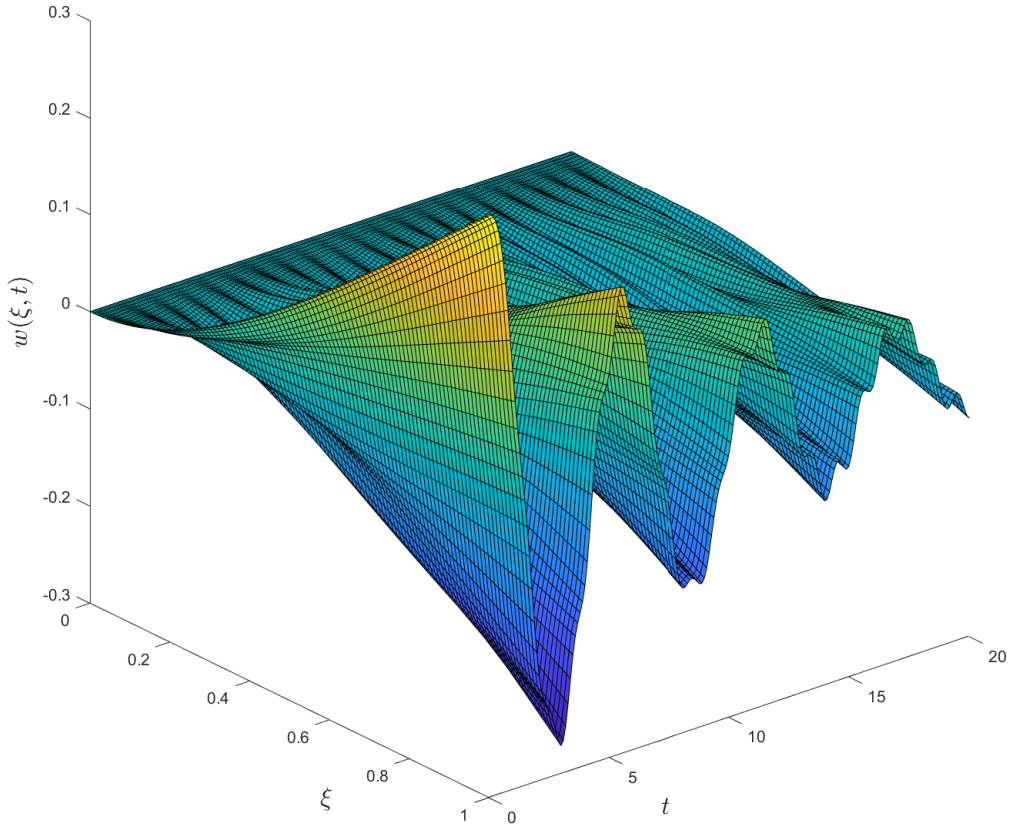

Figure 4.3. *A cantilevered beam with boundary control input* $\rho a \frac{\partial x_1}{\partial t}(0,t) = -\sin(2\pi t)$.

5 SATELLITE MODEL APPROXIMATION

In this chapter, we present a mathematical model for a satellite with two flexible solar panels and a rigid central body between them. The model we consider has been studied in, for example, [9] and [10]. We also express this interconnected system as a linear system of ordinary differential equations and how to simulate it, using the spectral Galerkin approach utilising the Legendre polynomials.

5.1 Satellite Model Setup

The three-component model we will use consists of a rigid central body and two flexible solar panels attached to it, opposite of each other. We model the central body as a dimensionless particle with mass m and moment of inertia I_m. The two solar panels are modelled as homogeneous, one-dimensional Euler–Bernoulli beams, being identical to each other. Their physical parameters are elastic modulus E, second moment of area I, cross-sectional area a, mass density ρ and viscous damping coefficient γ.

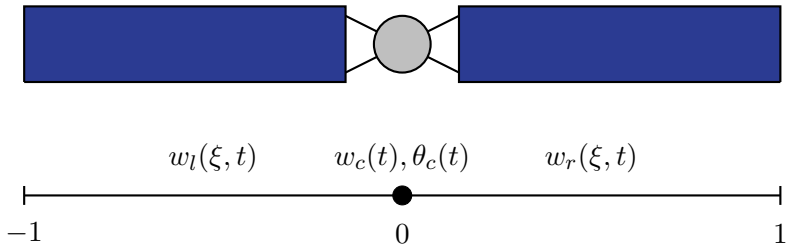

Figure 5.1. *A satellite with two flexible solar panels and a rigid central body.*

Let $w_l(\xi,t)$ and $w_r(\xi,t)$ denote the displacements of the left and right solar panels, respectively. Furthermore, let $w_c(t)$ and $\theta_c(t)$ denote the linear and angular displacements of the rigid central body. We can write the equations for the flexible solar panels as [9, Section 2]

$$\begin{cases} \dfrac{\partial^2 w_l}{\partial t^2}(\xi,t) + \dfrac{EI}{\rho a}\dfrac{\partial^4 w_l}{\partial \xi^4}(\xi,t) + \dfrac{\gamma}{\rho a}\dfrac{\partial w_l}{\partial t}(\xi,t) = 0, \quad -1 < \xi < 0, \quad t > 0, \\ \dfrac{\partial^2 w_r}{\partial t^2}(\xi,t) + \dfrac{EI}{\rho a}\dfrac{\partial^4 w_r}{\partial \xi^4}(\xi,t) + \dfrac{\gamma}{\rho a}\dfrac{\partial w_r}{\partial t}(\xi,t) = 0, \quad 0 < \xi < 1, \quad t > 0. \end{cases} \tag{5.1}$$

For the rigid central body, we have applied Newton's second law of motion to obtain [3,

p. 179]

$$\begin{cases} m\dfrac{d^2w_c}{dt^2}(t) = EI\dfrac{\partial^3 w_l}{\partial\xi^3}(0,t) - EI\dfrac{\partial^3 w_r}{\partial\xi^3}(0,t) + u_1(t), & t>0, \quad \text{(translation)} \\ I_m\dfrac{d^2\theta_c}{dt^2}(t) = -EI\dfrac{\partial^2 w_l}{\partial\xi^2}(0,t) + EI\dfrac{\partial^2 w_r}{\partial\xi^2}(0,t) + u_2(t), & t>0, \quad \text{(rotation)} \end{cases} \tag{5.2}$$

where u_1 and u_2 are the external inputs for the satellite system. Here we assume that there are no other forces or torques acting on the system. With this in mind, the only forces acting on the central body are the shear forces applied by the solar panels at $\xi = 0$. Similarly, the only torques affecting the central body come from the bending moments caused by the solar panels at $\xi = 0$. Moreover, our boundary conditions are

$$\begin{cases} \dfrac{\partial^2 w_l}{\partial\xi^2}(-1,t) = \dfrac{\partial^3 w_l}{\partial\xi^3}(-1,t) = 0, \\ \dfrac{\partial^2 w_r}{\partial\xi^2}(1,t) = \dfrac{\partial^3 w_r}{\partial\xi^3}(1,t) = 0, \\ \dfrac{dw_c}{dt}(t) = \dfrac{\partial w_l}{\partial t}(0,t) = \dfrac{\partial w_r}{\partial t}(0,t), \\ \dfrac{d\theta_c}{dt}(t) = \dfrac{\partial^2 w_l}{\partial\xi\partial t}(0,t) = \dfrac{\partial^2 w_r}{\partial\xi\partial t}(0,t). \end{cases} \tag{5.3}$$

The first two lines of boundary conditions describe the outer endpoints of the solar panels, which are modelled as free ends. The latter two boundary conditions link the velocity and angular velocity of the central body to the rate of change of the deflection and slope of the solar panels at $\xi = 0$.

We will not expand our analysis of the system further in this form. Instead, we express the two beam equations using the energy space variables and the spectral Galerkin approach to obtain two systems of ordinary differential equations in time. The equations of motion for the rigid central body already form a system of ordinary differential equations, so we can use $m\frac{dw_c}{dt}$ and $I_m\frac{d\theta_c}{dt}$ as state variables.

5.2 Finding Required Basis Functions

Using the energy variables for both of the solar panels, we denote

$$x_l(\xi,t) = \begin{bmatrix} x_l^1(\xi,t) \\ x_l^2(\xi,t) \end{bmatrix} = \begin{bmatrix} \rho a\frac{\partial w_l}{\partial t}(\xi,t) \\ \frac{\partial^2 w_l}{\partial\xi^2}(\xi,t) \end{bmatrix}, \qquad -1<\xi<0, \quad t>0 \tag{5.4}$$

$$x_r(\xi,t) = \begin{bmatrix} x_r^1(\xi,t) \\ x_r^2(\xi,t) \end{bmatrix} = \begin{bmatrix} \rho a\frac{\partial w_r}{\partial t}(\xi,t) \\ \frac{\partial^2 w_r}{\partial\xi^2}(\xi,t) \end{bmatrix}, \qquad 0<\xi<1, \quad t>0. \tag{5.5}$$

The approximate spectral Galerkin forms of these are

$$x_l^N(\xi,t) = \begin{bmatrix} x_{l1}^N(\xi,t) \\ x_{l2}^N(\xi,t) \end{bmatrix} = \begin{bmatrix} \sum_{n=0}^N \alpha_n^l(t)\phi_n^l(\xi) \\ \sum_{n=0}^N \beta_n^l(t)\Phi_n^l(\xi) \end{bmatrix}, \qquad -1 < \xi < 0, \quad t > 0 \tag{5.6}$$

$$x_r^N(\xi,t) = \begin{bmatrix} x_{r1}^N(\xi,t) \\ x_{r2}^N(\xi,t) \end{bmatrix} = \begin{bmatrix} \sum_{n=0}^N \alpha_n^r(t)\phi_n^r(\xi) \\ \sum_{n=0}^N \beta_n^r(t)\Phi_n^r(\xi) \end{bmatrix}, \qquad 0 < \xi < 1, \quad t > 0. \tag{5.7}$$

Additionally, we denote

$$\tilde{x}_l(t) \coloneqq \begin{bmatrix} \alpha_0^l(t) & \alpha_1^l(t) & \dots & \alpha_N^l(t) & \beta_0^l(t) & \beta_1^l(t) & \dots & \beta_N^l(t) \end{bmatrix}^\mathsf{T}, \tag{5.8}$$

$$\tilde{x}_r(t) \coloneqq \begin{bmatrix} \alpha_0^r(t) & \alpha_1^r(t) & \dots & \alpha_N^r(t) & \beta_0^r(t) & \beta_1^r(t) & \dots & \beta_N^r(t) \end{bmatrix}^\mathsf{T}, \tag{5.9}$$

$$x_c(t) \coloneqq \begin{bmatrix} m\frac{dw_c}{dt}(t) \\ I_m\frac{d\theta_c}{dt}(t) \end{bmatrix}, \tag{5.10}$$

which will be our state variables representing the solar panels and the central body in our approximated satellite system. We interconnect the three parts by defining inputs and outputs for them. For the left solar panel, we have [9, Section 2.1]

$$\begin{cases} u_l^1(t) = \dfrac{\partial w_l}{\partial t}(0,t), \\ u_l^2(t) = \dfrac{\partial^2 w_l}{\partial \xi \partial t}(0,t), \\ y_l^1(t) = -EI\dfrac{\partial^3 w_l}{\partial \xi^3}(0,t), \\ y_l^2(t) = EI\dfrac{\partial^2 w_l}{\partial \xi^2}(0,t). \end{cases} \tag{5.11}$$

Because $y_l^1(t) \approx -EI\sum_{n=0}^N \frac{d\Phi_n^l}{d\xi}(0)\beta_n^l(t)$ and $y_l^2(t) \approx EI\sum_{n=0}^N \Phi_n^l(0)\beta_n^l(t)$, we may express these in matrix–vector form as

$$u_l(t) = \begin{bmatrix} u_l^1(t) \\ u_l^2(t) \end{bmatrix}, \tag{5.12}$$

$$y_l(t) = \begin{bmatrix} y_l^1(t) \\ y_l^2(t) \end{bmatrix} \approx C_l\tilde{x}_l(t), \tag{5.13}$$

where

$$C_l = EI\begin{bmatrix} 0 & 0 & \cdots & 0 & -\frac{d\Phi_0^l}{d\xi}(0) & -\frac{d\Phi_1^l}{d\xi}(0) & \cdots & -\frac{d\Phi_N^l}{d\xi}(0) \\ 0 & 0 & \cdots & 0 & \Phi_0^l(0) & \Phi_1^l(0) & \cdots & \Phi_N^l(0) \end{bmatrix} \in \mathbb{R}^{2\times(2N+2)}. \tag{5.14}$$

Similarly for the right solar panel, we have

$$\begin{cases} u_r^1(t) = \dfrac{\partial w_r}{\partial t}(0,t), \\ u_r^2(t) = \dfrac{\partial^2 w_r}{\partial \xi \partial t}(0,t), \\ y_r^1(t) = EI\dfrac{\partial^3 w_r}{\partial \xi^3}(0,t), \\ y_r^2(t) = -EI\dfrac{\partial^2 w_r}{\partial \xi^2}(0,t), \end{cases} \tag{5.15}$$

which we can express as

$$u_r(t) = \begin{bmatrix} u_r^1(t) \\ u_r^2(t) \end{bmatrix}, \tag{5.16}$$

$$y_r(t) = \begin{bmatrix} y_r^1(t) \\ y_r^2(t) \end{bmatrix} \approx C_r \tilde{x}_r(t), \tag{5.17}$$

where

$$C_r = EI \begin{bmatrix} 0 & 0 & \cdots & 0 & \frac{d\Phi_0^r}{d\xi}(0) & \frac{d\Phi_1^r}{d\xi}(0) & \cdots & \frac{d\Phi_N^r}{d\xi}(0) \\ 0 & 0 & \cdots & 0 & -\Phi_0^r(0) & -\Phi_1^r(0) & \cdots & -\Phi_N^r(0) \end{bmatrix} \in \mathbb{R}^{2\times(2N+2)}. \tag{5.18}$$

For the rigid central body, we have [9, Section 2.3]

$$\begin{cases} u_f^1(t) = EI\dfrac{\partial^3 w_l}{\partial \xi^3}(0,t) - EI\dfrac{\partial^3 w_r}{\partial \xi^3}(0,t), \\ u_f^2(t) = -EI\dfrac{\partial^2 w_l}{\partial \xi^2}(0,t) + EI\dfrac{\partial^2 w_r}{\partial \xi^2}(0,t), \\ y_f^1(t) = \dfrac{dw_c}{dt}(t), \\ y_f^2(t) = \dfrac{d\theta_c}{dt}(t). \end{cases} \tag{5.19}$$

In the same vein, we can express these inputs and outputs as

$$u_f(t) = \begin{bmatrix} u_f^1(t) \\ u_f^2(t) \end{bmatrix}, \tag{5.20}$$

$$y_f(t) = \begin{bmatrix} y_f^1(t) \\ y_f^2(t) \end{bmatrix} = C_c x_c(t), \tag{5.21}$$

where

$$C_c = \begin{bmatrix} \frac{1}{m} & 0 \\ 0 & \frac{1}{I_m} \end{bmatrix} \in \mathbb{R}^{2\times 2}. \tag{5.22}$$

For the interconnections between the solar panels and the central body, for the homogeneous parts of the basis functions, we need the energy variables to satisfy

$$\begin{cases} \dfrac{1}{\rho a} x_l^1(0,t) = 0, \\ \dfrac{1}{\rho a}\dfrac{\partial x_l^1}{\partial \xi}(0,t) = 0, \\ x_l^2(-1,t) = 0, \\ \dfrac{\partial x_l^2}{\partial \xi}(-1,t) = 0, \end{cases} \tag{5.23}$$

for the left solar panel, and

$$\begin{cases} \dfrac{1}{\rho a} x_r^1(0,t) = 0, \\ \dfrac{1}{\rho a}\dfrac{\partial x_r^1}{\partial \xi}(0,t) = 0, \\ x_r^2(1,t) = 0, \\ \dfrac{\partial x_r^2}{\partial \xi}(1,t) = 0, \end{cases} \tag{5.24}$$

for the right solar panel. As covered in section 4.4, in terms of the spectral Galerkin modal basis functions, we need them to satisfy

$$\begin{cases} \phi_n^l(0) = 0, & n = 0,1,\ldots,N-2 \\ \dfrac{d\phi_n^l}{d\xi}(0) = 0, & n = 0,1,\ldots,N-2 \\ \Phi_n^l(-1) = 0, & n = 0,1,\ldots,N \\ \dfrac{d\Phi_n^l}{d\xi}(-1) = 0, & n = 0,1,\ldots,N \end{cases} \tag{5.25}$$

and

$$\begin{cases} \phi_n^r(0) = 0, & n = 0,1,\ldots,N-2 \\ \dfrac{d\phi_n^r}{d\xi}(0) = 0, & n = 0,1,\ldots,N-2 \\ \Phi_n^r(1) = 0, & n = 0,1,\ldots,N \\ \dfrac{d\Phi_n^r}{d\xi}(1) = 0, & n = 0,1,\ldots,N. \end{cases} \tag{5.26}$$

These make up the homogeneous part of the modal basis function sets. In order to apply boundary control for the interconnections, we require

$$\begin{cases} \phi_{N-1}^l(0) = 1, \\ \dfrac{d\phi_{N-1}^l}{d\xi}(0) = 0, \\ \phi_N^l(0) = 0, \\ \dfrac{d\phi_N^l}{d\xi}(0) = 1, \end{cases} \tag{5.27}$$

and

$$\begin{cases} \phi_{N-1}^r(0) = 1, \\ \dfrac{d\phi_{N-1}^r}{d\xi}(0) = 0, \\ \phi_N^r(0) = 0, \\ \dfrac{d\phi_N^r}{d\xi}(0) = 1. \end{cases} \tag{5.28}$$

We have developed our theory on Legendre polynomials and approximations with the domain $\Omega = [0, 1]$ in mind, but for ϕ_n^l and Φ_n^l, we need basis functions defined on $[-1, 0]$ instead. This is not a problem, as the boundary conditions we have for the basis functions for the left and right solar panels are symmetric about $\xi = 0$. This means, for example, that when we find basis functions $\Phi_n^r(\xi)$ satisfying $\Phi_n^r(1) = \frac{d\Phi_n^r}{d\xi}(1) = 0$ on $[0, 1]$, functions $\Phi_n^r(-\xi)$ satisfy $\Phi_n^r(-1) = \frac{d\Phi_n^r}{d\xi}(-1) = 0$ on $[-1, 0]$. Thus if we know Φ_n^r, we can use Φ_n^l defined as $\Phi_n^l(\xi) = \Phi_n^r(-\xi)$ on $[-1, 0]$ for the left solar panel. Similarly, first solving for ϕ_n^r, we can use ϕ_n^l defined as $\phi_n^l(\xi) = \phi_n^r(-\xi)$ on $[-1, 0]$ for the left solar panel.

For the right solar panel, our boundary conditions in (5.26) are equivalent to

$$W_r' \begin{bmatrix} \mathcal{H} & & & \\ & \mathcal{H} & & \\ & & \mathcal{H} & \\ & & & \mathcal{H} \end{bmatrix} \begin{bmatrix} \phi_n^r(1) \\ \Phi_n^r(1) \\ \frac{d\phi_n^r}{d\xi}(1) \\ \frac{d\Phi_n^r}{d\xi}(1) \\ \phi_n^r(0) \\ \Phi_n^r(0) \\ \frac{d\phi_n^r}{d\xi}(0) \\ \frac{d\Phi_n^r}{d\xi}(0) \end{bmatrix} = \begin{bmatrix} 0 \\ 0 \\ 0 \\ 0 \end{bmatrix} \tag{5.29}$$

with

$$W_r' = \begin{bmatrix} 0 & 1 & 0 & 0 & 0 & 0 & 0 & 0 \\ 0 & 0 & 0 & 1 & 0 & 0 & 0 & 0 \\ 0 & 0 & 0 & 0 & 1 & 0 & 0 & 0 \\ 0 & 0 & 0 & 0 & 0 & 0 & 1 & 0 \end{bmatrix}. \tag{5.30}$$

Denoting

$$\begin{cases} \phi_n^r(\xi) = L_n(\xi) + \sum_{k=1}^{4} g_k^{1,r}(n) L_{n+k}(\xi), \\ \Phi_n^r(\xi) = L_n(\xi) + \sum_{k=1}^{4} g_k^{2,r}(n) L_{n+k}(\xi), \\ g_r^1(n) = \begin{bmatrix} 1 & g_1^{1,r}(n) & g_2^{1,r}(n) & g_3^{1,r}(n) & g_4^{1,r}(n) \end{bmatrix}^\mathsf{T}, \\ g_r^2(n) = \begin{bmatrix} 1 & g_1^{2,r}(n) & g_2^{2,r}(n) & g_3^{2,r}(n) & g_4^{2,r}(n) \end{bmatrix}^\mathsf{T}, \end{cases} \tag{5.31}$$

we are ready to solve (4.58) (with $C_n = I_{2\times 2}$). We can eliminate the physical parameters ρa and EI from the system by multiplying (4.58) by $\operatorname{diag}\left(\frac{1}{EI}, \frac{1}{EI}, \rho a, \rho a\right)$ from the left. Our system becomes

$$W_r' \begin{bmatrix} \Lambda_n(1) & 0 \\ 0 & \Lambda_n(1) \\ \Lambda_n'(1) & 0 \\ 0 & \Lambda_n'(1) \\ \Lambda_n(0) & 0 \\ 0 & \Lambda_n(0) \\ \Lambda_n'(0) & 0 \\ 0 & \Lambda_n'(0) \end{bmatrix} \begin{bmatrix} g^1(n) \\ g^2(n) \end{bmatrix} = \begin{bmatrix} 0 \\ 0 \\ 0 \\ 0 \end{bmatrix}, \tag{5.32}$$

where Λ_n and Λ_n' are described in (4.55) and (4.56). One solution to this system is

$$g_1^{1,r}(n) = \frac{2n+3}{n+2}, \qquad g_2^{1,r}(n) = \frac{n+1}{n+2}, \qquad g_3^{1,r}(n) = 0, \qquad g_4^{1,r}(n) = 0,$$
$$g_1^{2,r}(n) = -\frac{2n+3}{n+2}, \qquad g_2^{2,r}(n) = \frac{n+1}{n+2}, \qquad g_3^{2,r}(n) = 0, \qquad g_4^{2,r}(n) = 0,$$

which lacks the higher degree terms L_{n+3} and L_{n+4} as desired. For ϕ_{N-1}^r and ϕ_N^r, we look for linear combinations of L_0, L_1 and L_2 that satisfy (5.28). For example, we can use

$$\begin{cases} \phi_{N-1}^r(\xi) = -\frac{3}{2}L_1(\xi) - \frac{1}{2}L_2(\xi) = -3\xi^2 + 1, \\ \phi_N^r(\xi) = -\frac{1}{4}L_1(\xi) - \frac{1}{4}L_2(\xi) = -\frac{3}{2}\xi^2 + \xi, \end{cases} \tag{5.33}$$

which satisfy (5.28) and $\int_0^1 \phi_{N-1}^r(\xi)\, d\xi = \int_0^1 \phi_N^r(\xi)\, d\xi = 0$. For the right solar panel, we

have the basis functions

$$\begin{cases} \phi_n^r(\xi) = L_n(\xi) + \dfrac{2n+3}{n+2}L_{n+1}(\xi) + \dfrac{n+1}{n+2}L_{n+2}(\xi), & n = 0, 1, \ldots, N-2, \\ \phi_{N-1}^r(\xi) = -3\xi^2 + 1, \\ \phi_N^r(\xi) = -\dfrac{3}{2}\xi^2 + \xi, \\ \Phi_n^r(\xi) = L_n(\xi) - \dfrac{2n+3}{n+2}L_{n+1}(\xi) + \dfrac{n+1}{n+2}L_{n+2}(\xi), & n = 0, 1, \ldots, N, \end{cases}$$

for $\xi \in [0, 1]$. One can verify that these satisfy the required boundary conditions. Because of the symmetry of the boundary conditions discussed earlier, for the left solar panel, we get the basis functions

$$\begin{cases} \phi_n^l(\xi) = L_n(-\xi) + \dfrac{2n+3}{n+2}L_{n+1}(-\xi) + \dfrac{n+1}{n+2}L_{n+2}(-\xi), & n = 0, 1, \ldots, N-2, \\ \phi_{N-1}^l(\xi) = -3\xi^2 + 1, \\ \phi_N^l(\xi) = \dfrac{3}{2}\xi^2 + \xi, \\ \Phi_n^l(\xi) = L_n(-\xi) - \dfrac{2n+3}{n+2}L_{n+1}(-\xi) + \dfrac{n+1}{n+2}L_{n+2}(-\xi), & n = 0, 1, \ldots, N, \end{cases}$$

for $\xi \in [-1, 0]$, which again one can verify to satisfy the required boundary conditions.

5.3 Satellite Model as a Linear Matrix System

Having found the necessary spectral Galerkin modal basis functions, we can construct the matrix model of the satellite. Because the model components internally control the values of $x_l^1(0,t)$, $\frac{\partial x_l^1}{\partial \xi}(0,t)$, $x_r^1(0,t)$ and $\frac{\partial x_r^1}{\partial \xi}(0,t)$ and we have no boundary control input involving x_l^2 and x_r^2, we use formulations described in section 4.4 for both the left and right solar panels. For the left solar panel, we replace $\xi = 0$ with $\xi = -1$ and $\xi = 1$ with $\xi = 0$ in the formulations. Additionally, for the left solar panel, we use the L^2-inner product computed over the interval $[-1, 0]$ instead.

We can write equation (4.40) with the outputs for the solar panels as

$$\begin{cases} M_l \dfrac{d}{dt}\tilde{x}_l(t) = K_l\tilde{x}_l(t) + B_l u_l(t), & t > 0, \\ \tilde{x}_l(0) = \tilde{x}_0^l \in \mathbb{R}^{2N+2}, \\ y_l(t) = C_l\tilde{x}_l(t), \end{cases} \tag{5.34}$$

and

$$\begin{cases} M_r \dfrac{d}{dt}\tilde{x}_r(t) = K_r \tilde{x}_r(t) + B_r u_r(t), \qquad t > 0, \\ \tilde{x}_r(0) = \tilde{x}_0^r \in \mathbb{R}^{2N+2}, \\ y_r(t) = C_r \tilde{x}_r(t), \end{cases} \tag{5.35}$$

where M_l and M_r are as in (4.13),

$$K_l = \begin{bmatrix} K_1^l & K_2^l \\ 0 & K_3^l \end{bmatrix}, \qquad B_l = \begin{bmatrix} 0 \\ B_2^l \end{bmatrix} = \frac{1}{\rho a} \begin{bmatrix} 0 & 0 \\ \vdots & \vdots \\ 0 & 0 \\ -\frac{d\Phi_0^l}{d\xi}(0) & \Phi_0^l(0) \\ \vdots & \vdots \\ -\frac{d\Phi_N^l}{d\xi}(0) & \Phi_N^l(0) \end{bmatrix}, \qquad u_l(t) = \begin{bmatrix} u_l^1(t) \\ u_l^2(t) \end{bmatrix},$$

$$K_r = \begin{bmatrix} K_1^r & K_2^r \\ 0 & K_3^r \end{bmatrix}, \qquad B_r = \begin{bmatrix} 0 \\ B_2^r \end{bmatrix} = \frac{1}{\rho a} \begin{bmatrix} 0 & 0 \\ \vdots & \vdots \\ 0 & 0 \\ \frac{d\Phi_0^r}{d\xi}(0) & -\Phi_0^r(0) \\ \vdots & \vdots \\ \frac{d\Phi_N^r}{d\xi}(0) & -\Phi_N^r(0) \end{bmatrix}, \qquad u_r(t) = \begin{bmatrix} u_r^1(t) \\ u_r^2(t) \end{bmatrix}.$$

Computing the mass and stiffness matrices involves computing the L^2-inner products between the basis functions and their second derivatives. While these can be computed analytically using property (iv) of Legendre polynomials, Theorem 2.7 and using the substitution $\xi' = -\xi$ for the left solar panel, we will not do that due to the complexity of the formulas involved. In practice, one can apply these formulas in a computer algorithm or compute the inner products using numerical integration. For the rigid central body, we can write

$$\begin{cases} \dfrac{d}{dt} x_c(t) = u_f(t) + u(t), \qquad t > 0, \\ x_c(0) = x_0^c \in \mathbb{R}^2, \\ y_f(t) = C_c x_c(t), \end{cases} \tag{5.36}$$

where $u(t) = \begin{bmatrix} u_1(t) & u_2(t) \end{bmatrix}^\mathsf{T}$ is the external output to the system. Finally, we can interconnect the three systems. First, we collect the connections between our internal component inputs and outputs

$$\begin{cases} u_l(t) = y_f(t) = C_c x_c(t), \\ u_r(t) = y_f(t) = C_c x_c(t), \\ u_f(t) = -\big(y_l(t) + y_r(t)\big) = -\big(C_l \tilde{x}_l(t) + C_r \tilde{x}_r(t)\big). \end{cases} \tag{5.37}$$

Applying these connections, we obtain

$$\begin{cases} M_l \dfrac{d}{dt}\tilde{x}_l(t) = K_l\tilde{x}_l(t) + B_l C_c x_c(t) \\ M_r \dfrac{d}{dt}\tilde{x}_r(t) = K_r\tilde{x}_r(t) + B_r C_c x_c(t) \\ \dfrac{d}{dt}x_c(t) = -\big(C_l\tilde{x}_l(t) + C_r\tilde{x}_r(t)\big) + u(t), \\ y(t) = x_c(t). \end{cases} \tag{5.38}$$

We can write the complete system with output as

$$\begin{cases} M_s \dfrac{d}{dt}x_s(t) = K_s x_s(t) + B_s u_s(t), \qquad t > 0, \\ x_s(0) = x_0^s, \\ y(t) = C_s x_s(t), \end{cases} \tag{5.39}$$

where

$$M_s = \begin{bmatrix} M_l & 0 & 0 \\ 0 & M_r & 0 \\ 0 & 0 & I \end{bmatrix}, \qquad K_s = \begin{bmatrix} K_l & 0 & B_l C_c \\ 0 & K_r & B_r C_c \\ -C_l & -C_r & 0 \end{bmatrix}, \qquad B_s = \begin{bmatrix} 0 & 0 & 0 \\ 0 & 0 & 0 \\ 0 & 0 & I \end{bmatrix},$$

$$x_s(t) = \begin{bmatrix} \tilde{x}_l(t) \\ \tilde{x}_r(t) \\ x_c(t) \end{bmatrix}, \qquad x_0^s = \begin{bmatrix} \tilde{x}_0^l \\ \tilde{x}_0^r \\ x_0^c \end{bmatrix}, \qquad u_s(t) = \begin{bmatrix} 0 \\ 0 \\ u(t) \end{bmatrix},$$

and C_s is a linear operator depending on what we want as the output. We can write (5.39) in standard linear control system form as

$$\begin{cases} \dfrac{d}{dt}x_s(t) = \tilde{A}_s x_s(t) + \tilde{B}_s u_s(t), \qquad t > 0, \\ x_s(0) = x_0^s, \\ y(t) = C_s x_s(t), \end{cases} \tag{5.40}$$

where $\tilde{A}_s = M_s^{-1}K_s$ and $\tilde{B}_s = M_s^{-1}B_s$. We can do this because M_s is invertible, being a block diagonal matrix whose diagonal entries are invertible. Most numerical solvers for systems of ordinary differential equations, such as those in MATLAB, accept a mass matrix as an argument. Using formulation (5.39), we do not have to compute $M_s^{-1}K_s$ and $M_s^{-1}B_s$, which are prone to numerical errors. The latter formulation can be useful for analysing the system, such as studying the eigenvalues of $\tilde{A}$ or implementing a controller for the system. We do not cover these in this work.

5.4 Simulation Example for a Flexible Satellite

We simulate a flexible satellite with physical parameters $E = 1$, $I = 1$, $\rho = 2$, $a = 1$ and $\gamma = 2$ for the identical, flexible solar panels. For the rigid central body, our physical parameters are $m = 1$ and $I_m = 1$. Similarly to the cantilevered beam simulation in the previous chapter, we use 15 basis functions ϕ_n^l, Φ_n^l, ϕ_n^r and Φ_n^r for simulating both solar panels. We simulate the satellite for 20 seconds.

For the rigid central body, our initial conditions are $\frac{dw_c}{dt}(0) = 0$ and $\frac{d\theta_c}{dt}(0) = -1$. The solar panels are initially at rest with symmetric deflection profiles of

$$\begin{cases} w_l(\xi, 0) = \dfrac{1}{10}\big(\xi^4 + 4\xi^2 + 6\xi^2\big), & -1 < \xi < 0, \\ w_r(\xi, 0) = \dfrac{1}{10}\big(\xi^4 - 4\xi^2 + 6\xi^2\big), & 0 < \xi < 1. \end{cases} \tag{5.41}$$

These translate to the following initial conditions in terms of the energy variables:

$$\begin{cases} x_1^l(\xi, 0) = \rho a \dfrac{\partial w_l}{\partial t}(\xi, 0) \equiv 0, & -1 < \xi < 0, \\ x_2^l(\xi, 0) = \dfrac{\partial^2 w_l}{\partial \xi^2}(\xi, 0) = \dfrac{1}{10}\big(12\xi^2 + 24\xi + 12\big), & -1 < \xi < 0, \\ x_1^r(\xi, 0) = \rho a \dfrac{\partial w_r}{\partial t}(\xi, 0) \equiv 0, & 0 < \xi < 1, \\ x_2^r(\xi, 0) = \dfrac{\partial^2 w_r}{\partial \xi^2}(\xi, 0) = \dfrac{1}{10}\big(12\xi^2 - 24\xi + 12\big), & 0 < \xi < 1. \end{cases} \tag{5.42}$$

For the simulation, we again solve for the basis function coefficients for the spectral approximations in (5.6) and (5.7) at $t = 0$ to obtain the initial condition in terms of these coefficients. We simulate the satellite both with zero inputs to the central body and with inputs $u_1(t) = -\cos(2\pi t)$ and $u_2(t) = \frac{1}{4}\sin(\pi t)$. The linear and angular velocities of the central body are shown in figures 5.2 and 5.3, respectively. Likewise, the deflection profile of the two flexible solar panels are shown in figures 5.4 and 5.5, respectively.

We see that without control input, the rigid central body reaches a stable state, as $\frac{dw_c}{dt}$ and $\frac{d\theta_c}{dt}$ are approaching zero towards the end of our 20-second simulation. On the other hand, with the periodic control inputs, $\frac{dw_c}{dt}$ and $\frac{d\theta_c}{dt}$ approach periodic oscillation of constant amplitude and frequency, centered at zero. These frequencies match the frequencies of our input functions.

Similarly to the rigid central body, with no control input, the flexible solar panels reach a stable state towards the end of our simulation. The solar panels rotate counterclockwise due to the initial angular velocity of the central body being negative. With the periodic control input applied, the solar panels approach a similar orientation, but with periodic oscillation of constant amplitude and frequency.

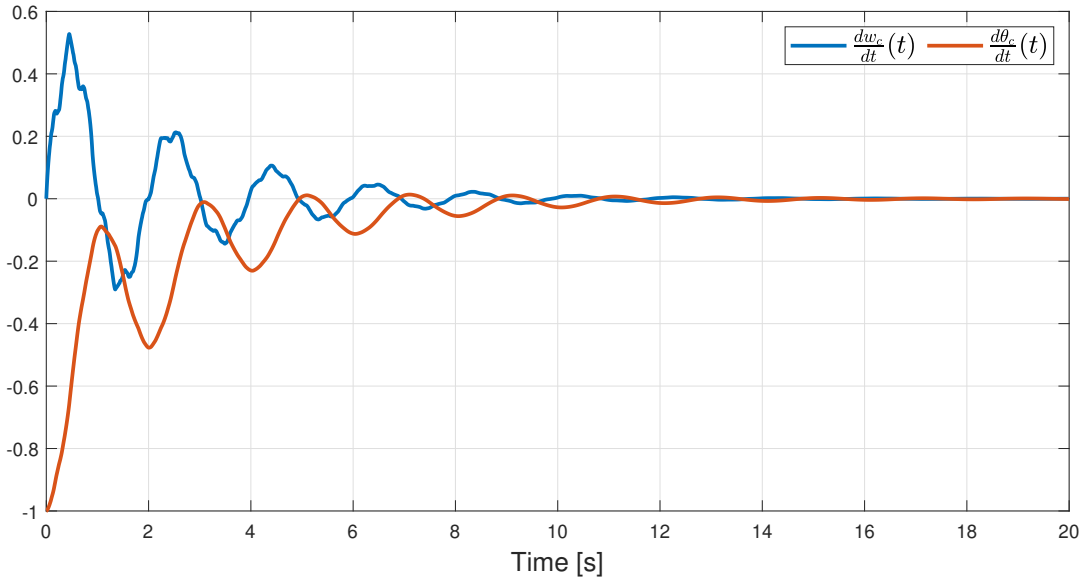

Figure 5.2. *The rigid central body satellite without control inputs.*

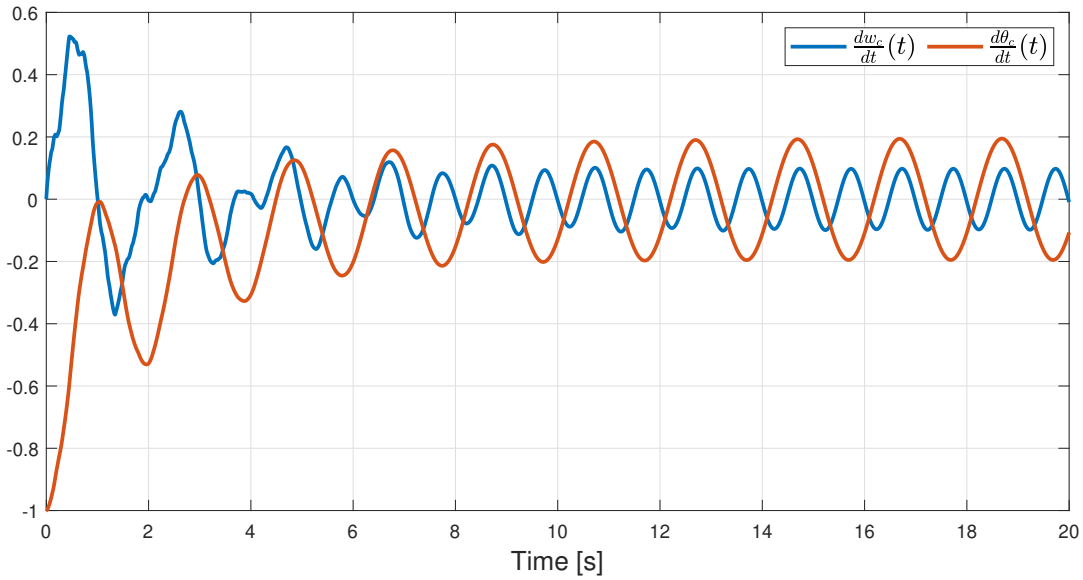

Figure 5.3. *The rigid central body with control input functions* $u_1(t) = -\cos(2\pi t)$ *and* $u_2(t) = \frac{1}{4}\sin(\pi t)$.

5.5 Matlab Codes for the Satellite Approximation

All the codes used for simulating a single beam and the satellite approximation are available online in the writer's GitHub repository. Documentation is not provided, but the files are commented in such a way that they should be easy to understand after reading this work. The files are openly accessible at `https://github.com/Kristian-MJA/Satmodel`.

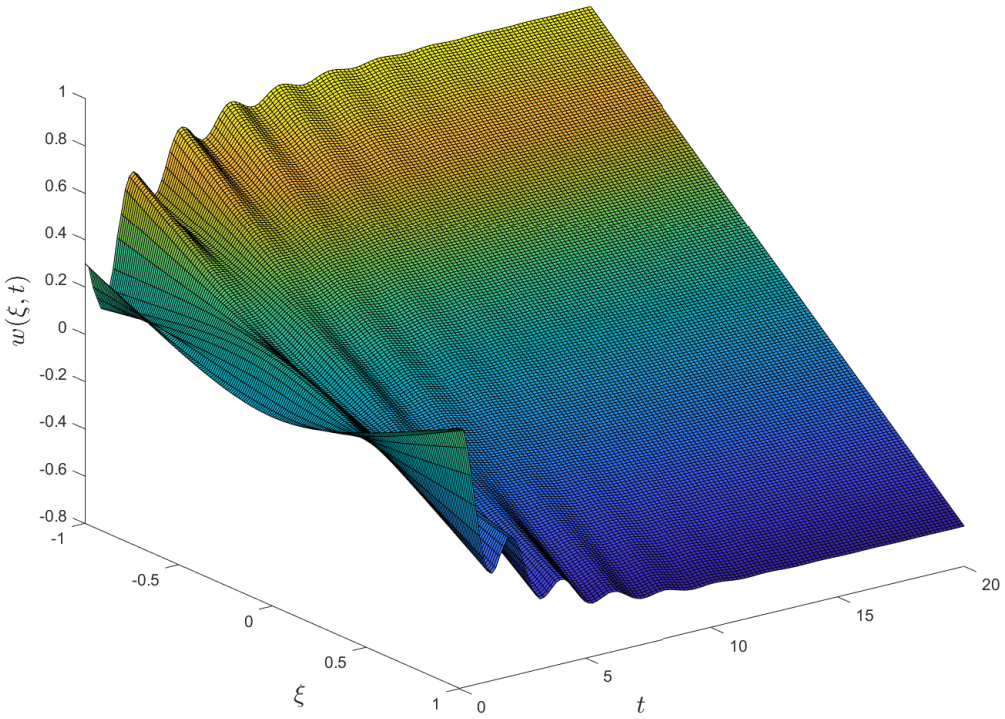

Figure 5.4. *The two flexible solar panels with no control inputs.*

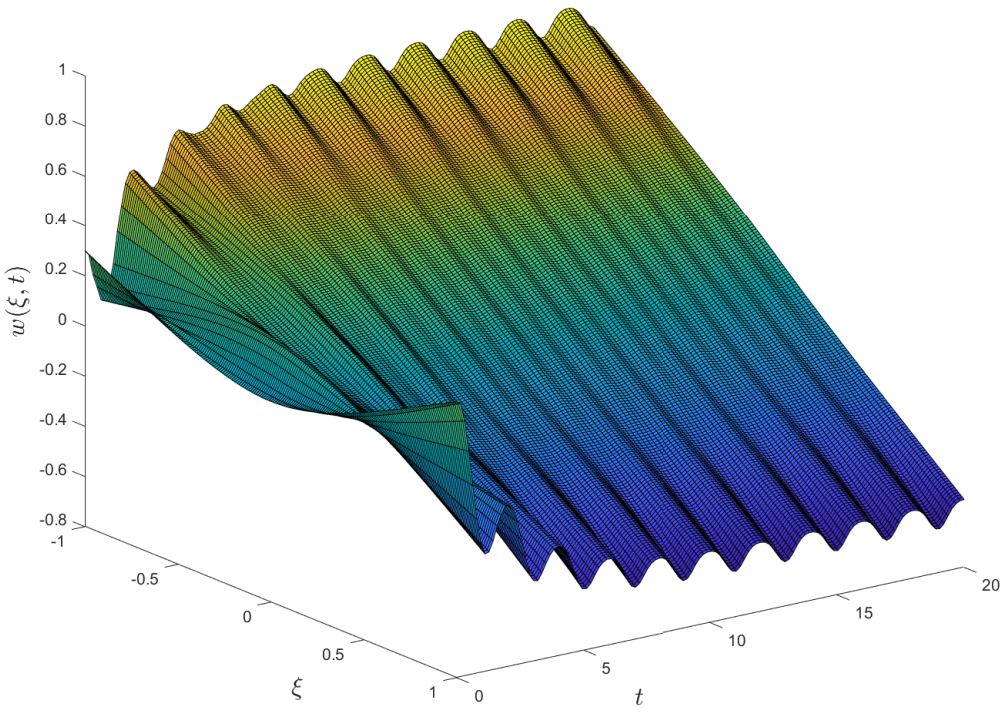

Figure 5.5. *The two flexible solar panels with control input functions* $u_1(t) = -\cos(2\pi t)$ *and* $u_2(t) = \frac{1}{4}\sin(\pi t)$.

6 CONCLUSIONS

In this work, we developed a numerical approximation method for simulating dynamic Euler–Bernoulli beams. We also used the model to simulate a flexible satellite, which is made of two flexible solar panels and a rigid central body. The solar panels are modelled as Euler–Bernoulli beams and the central body is modelled as a system of two ordinary differential equations. Using the developed models, we simulated both a single beam and a flexible satellite using MATLAB.

From the beginning, the approximate beam model was developed with the possibility of applying boundary control input. Even if one does not need time-dependent boundary conditions, the model is still applicable, as this corresponds to constant boundary input. The starting point for the model was to transform the original fourth order partial differential equation describing an Euler–Bernoulli beam into a system of two new partial differential equations, which are both first order in time, by introducing two new variables. This allowed us to apply the theory developed for linear control theory, which considers first-order abstract differential equations. With these tools, we were able to study the existence of solutions to the beam equation equipped with homogeneous boundary conditions.

The largest part of this work was dedicated to developing the approximate model for a single Euler–Bernoulli beam. We achieved this by applying weighted residual methods and considering weak solutions to the new system of two partial differential equations. We chose to apply the spectral Galerkin method for approximating the new variables with finite linear combinations of so-called modal basis functions constructed from Legendre polynomials. Proceeding from there, we performed semidiscretisation on the weak formulation of the new system, in order to obtain linear system of ordinary differential equations, which can be solved with various solvers developed for ordinary differential equations. We also developed a method for determining the required modal basis functions, which depend on the boundary conditions of the beam equation.

The main goal of this work was to apply the developed approximate beam model for a flexible satellite model. As the three components of the satellite model are connected to each other via boundary, inclusion of boundary control inputs was essential. We combined the three systems of ordinary differential equations describing the flexible satellite into a single, larger system which can then be solved numerically. We included control inputs to the system via the central body. We were interested in solving for the linear and angular velocities of the central body of the satellite body and the deflection profile of the

solar panels. Future extensions to our satellite model would be implementing a controller to move and rotate the satellite to a specific orientation and to stabilise the vibrations of the solar panels. For example, we might require a satellite to have the same side facing towards Earth at all times while orbiting around the planet.

In general, the approximate beam model could be extended to structures consisting of several Euler–Bernoulli beams that are connected to each other via the boundary. A simple example would be having N beams connected in series. Another application could be modelling the wind turbine in a wind power plant, which has usually three identical blades connected to the centre. The turbine blades are long and massive enough to vibrate during the rotation of the turbine. Being able to simulate the vibrations caused by the turbine blades could be helpful in designing of new wind power plants. However, as our beam model is limited to homogeneous beams, the turbine blades need to be sufficiently homogeneous along their length. Unlike with a satellite in space, we would, in addition, need to take air resistance into account.

Indeed, the most clear shortcoming of our approximate beam model is that it is limited to homogeneous beams. Several real life beams are inhomogeneous, so extending our model to allow for inhomogeneous beams would be a definite improvement. However, this would require deriving many of our formulations differently, as the physical parameters depend on location instead of being constant. This makes the beam equation more difficult to analyse and manipulate, and we might need to use different state variables when deriving the approximate system. This would likely make the final model very different and possibly harder to solve.

REFERENCES

[1] Agarwal, R. P. and O'Regan, D. *Ordinary and Partial Differential Equations With Special Functions, Fourier Series, and Boundary Value Problems*. Springer, 2009.

[2] Augner, B. and Jacob, B. Stability and Stabilization of Infinite-dimensional Linear Port-Hamiltonian Systems. *Evol. Equ. Control Theory* 3.2 (2014), 207–229.

[3] Bontsema, J., Curtain, R. and Schumacher, J. Robust Control of Flexible Structures: A Case Study. *Automatica* 24.2 (1988), 177–186.

[4] Doman, B. G. S. *The Classical Orthogonal Polynomials*. World Scientific, 2015.

[5] Engel, K.-J. and Nagel, R. *A Short Course on Operator Semigroups*. Springer, 2006.

[6] Gekeler, E. W. *Mathematical Methods for Mechanics : A Handbook with MATLAB Experiments*. Springer, 2008.

[7] Gere, J. M. and Goodno, B. J. *Mechanics of Materials Brief Edition*. Cengage Learning, 2012.

[8] Gorrec, Y. L., Zwart, H. and Masche, B. Dirac Structures and Boundary Control Systems Associated with Skew-symmetric Differential Operators. *SIAM J. Control Optim.* 44.5 (2005), 1864–1892.

[9] Govindaraj, T., Humaloja, J.-P. and Paunonen, L. Robust Output Regulation of a Flexible Satellite. *Proceedings of IFAC World Congress (Berlin, Germany, July 12–17, 2020)*. 2020.

[10] He, W. and Ge, S. Dynamic Modeling and Vibration Control of a Flexible Satellite. *IEEE Transactions on Aerospace and Electronic Systems* 51 (Apr. 2015), 1422–1431.

[11] Hillen, T., Roessel, H. van and Leonard, I. E. *Partial Differential Equations : Theory and Completely Solved Problems*. John Wiley & Sons, Incorporated, 2012.

[12] Jacob, B. and Zwart, H. J. *Linear Port-Hamiltonian Systems on Infinite-dimensional Spaces*. Birkhäuser, 2012.

[13] Luo, Z.-H., Guo, B.-Z. and Morgul, O. *Stability and Stabilization of Infinite Dimensional Systems with Applications*. Springer, 1999.

[14] Rynne, B. P. and Youngson, M. A. *Linear Functional Analysis : Second Edition*. Springer, 2008.

[15] Shen, J. Efficient Spectral-Galerkin Method I. Direct Solvers for the Second and Fourth Order Equations Using Legendre Polynomials. *SIAM J. Sci. Comput.* 15.6 (1994), 1489–1505.

[16] Shen, J. Efficient Spectral-Galerkin Method II. Direct Solvers for the Second and Fourth Order Equations Using Chebyshev Polynomials. *SIAM J. Sci. Comput.* 16.1 (1995), 74–87.

[17] Shen, J., Tang, T. and Wang, L.-L. *Spectral Methods Algorithms, Analysis and Applications*. Springer, 2011.